AN ANALOG COMPUTER STUDY OF HYDRAULIC SERVOMECHANISM NONLINEARITIES

by

Keith A. Erikson, 1st Lieutenant, USAF
B.S.M.E., Kansas State College, 1952

William R. Greenwood, 1st Lieutenant, USAF
B.S.E.E., Purdue University, 1952

Philip J. Bonomo, 1st Lieutenant, USAF
B.S.E.E., Purdue University, 1952

SUBMITTED IN PARTIAL FULFILLMENT OF THE
REQUIREMENTS FOR THE DEGREE OF
MASTER OF SCIENCE
at the
MASSACHUSETTS INSTITUTE OF TECHNOLOGY
1954

Signature of Authors

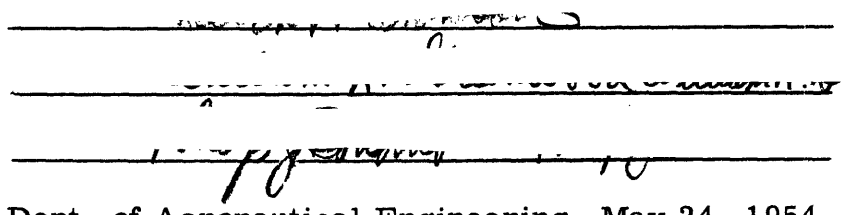

Dept. of Aeronautical Engineering, May 24, 1954

Certified by _____
Thesis Supervisor

_____
Chairman, Departmental Committee on Graduate Students

This thesis, written by the authors while affiliated with the Instrumentation Laboratory, M.I.T., has been reproduced by the offset process using printer's ink in accordance with the following basic authorization received by Dr. C. S. Draper, Director of the Instrumentation Laboratory.

COPY

April 7, 1950

Dr. C. S. Draper
33-103

Dear Dr. Draper:

Mr. L. E. Payne has shown to me a recent printed reproduction of a thesis, in this instance a Master's dissertation, submitted in partial fulfillment of the requirements for the degree of Master of Science at the Massachusetts Institute of Technology.

The sample shown is printed by the offset press using screened illustrations, graphs and other material. For the purposes of the Library which include record and permanent preservation, theses reproduced in this manner are perfectly satisfactory and in my opinion meet all of the physical requirements of the graduate school insofar as they pertain to the preparation of a thesis.

I note that in the sample submitted the signatures have been reproduced along with the text by photo lithography. It is suggested that for the Library record copy the author, thesis supervisor and chairman of the Departmental Committee on Graduate Students affix their signatures in writing as complete authorization of the study. These can be written above the reproduced signature if desired.

Sincerely yours,

(signed)

Vernon D. Tate
Director of Libraries

VDT/jl

cc: Dean Bunker
Mr. Payne

COPY

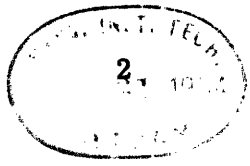

AN ANALOG COMPUTER STUDY OF HYDRAULIC SERVOMECHANISM NONLINEARITIES

by

Keith A. Erikson
William R. Greenwood
Philip J. Bonomo

Submitted to the Department of Aeronautical Engineering on May 24, 1954, in partial fulfillment of the requirements for the degree of Master of Science.

ABSTRACT

As the speed of modern aircraft becomes more extreme, the need for low apparatus-to-horsepower control equipment, an intrinsic property of hydraulic servomechanisms, becomes more acute. Consequently, the inherent nonlinearities of the hydraulic control medium have assumed an important role; generally because of their deleterious effects on system performance, but in certain particular situations, because they can be utilized to some advantage.

In this report, the operation of a nonlinear elevator control system is studied with an analog computer; the effects of nonlinear elements are tabulated for different load conditions and system parameters.

It was found that some nonlinearities could be neglected for certain specified operating conditions. These operating conditions are stated, and the changes in system performance with variations of load and system parameters are recorded.

The main conclusion reached is that the transfer characteristic of the valve must be reproduced very accurately for any extensive investigation of the hydraulic servo, even though some of the other nonlinear

elements such as coulomb friction may at times be safely ignored.

Thesis Supervisor:	Walter Wrigley
Title:	Associate Professor of Aeronautical Engineering

May 24, 1954

Professor Leicester F. Hamilton
Secretary of the Faculty
Massachusetts Institute of Technology
Cambridge 39, Massachusetts

Dear Professor Hamilton:

In accordance with the regulations of the faculty, we hereby submit a thesis entitled An Analog Computer Study of Hydraulic Servomechanism Nonlinearities in partial fulfillment of the requirements for the degree of Master of Science.

Keith A Erikson

William R. Greenwood

Philip J. Bonomo

ACKNOWLEDGEMENT

The authors wish to express their sincere appreciation to the personnel of the Instrumentation Laboratory, Massachusetts Institute of Technology, who have helped make this study possible. Special thanks are due to Dr. Walter Wrigley who, as thesis supervisor, inspired and guided the entire project, and to Phil Lapp and Ken Garnjost for their continuous interest, patience, and encouragement. To Messrs. Sam Giser and Frank S. Spada, our sincerest gratitude for their indispensable, yet convivial, assistance on the experimental aspect of the problem. And finally, to the librarians of the Instrumentation Laboratory Library and to all of the MIT Technical Publications Division who patiently assisted in the reproduction of this work, our warmest thanks.

The graduate work for which this thesis is a partial requirement was performed while the authors were assigned by the U.S. Air Force Institute of Technology for graduate study at the Massachusetts Institute of Technology. The thesis was prepared under the auspices of DIC Project 7139, sponsored by the Armament Laboratory of the Wright Air Development Center, through USAF Contract AF 33(616)-2039.

TABLE OF CONTENTS

OBJECT

This report endeavors to examine the nonlinearities in an aircraft elevator position control system, and to study the effects of the nonlinear elements upon overall system performance. In particular, the operating conditions under which the nonlinear effects are either emphasized or minimized are to be determined.

CHAPTER I

INTRODUCTION

A. General

The increased use of automatic flight control systems in recent years has resulted in a corresponding increase in the utilization of hydraulically actuated servomechanisms. Used in combination with electrical devices hydraulic servos possess many advantages over purely electromechanical systems (the more important of these, from the automatic flight control engineer's point of view, being the low apparatus-to-horsepower ratio and relatively rapid response time inherent in hydraulic servos)[1*]. Furthermore, the increasing emphasis on transonic and supersonic aircraft has made the utilization of powered flight control systems almost mandatory; such aircraft develop center of pressure shifts that cause extremely large control forces, and the maneuverability requirements are such as to make human response time a limiting factor[2]. Hence, the obvious need exists for automatic systems of high power amplification for utilization in such aircraft; again, electro-hydraulic servos are most advantageously utilized in such applications.

While the need for hydraulic servo analysis and synthesis may be obvious, hydraulic servos remain inherently nonlinear and, since "contemporary control system analysis...deviates with reluctance from the original concept of the completely linear system"[3], this feature of the hydraulic servo may well be regarded as a "stumbling block" in the full utilization of its capabilities. An objective of this report thus becomes a hope that the versatility of the analogue computer may help

---

* Superscript numbers refer to reference numbers of Bibliography (Appendix C)

overcome those factors that contribute to the quoted reluctance towards hydraulic servomechanism analysis and synthesis.

The present uses and future needs of hydraulic servos are of themselves sufficient incentives for extended study and analysis of these systems. However, the very characteristics that tend to discourage full utilization of these systems (i.e., their inherent nonlinearities) are added incentives towards their study. It has been pointed out in the literature that there are fundamental limitations on the refinements and improvements that are possible in purely linear systems[4]. While the accuracy and response time of linear servos have been greatly improved over the years (primarily from improvements of servo motors and controllers), it appears that such improvements have nearly reached the crest of their development. As demonstrated in the aforementioned reference, the use of nonlinear elements is then the next logical step in obviating the fundamental limitations on improved linear system design. In fact, it appears that "servo analysis of the future may be directed principally toward introducing nonlinear elements as means of optimizing control systems, in contrast to the present emphasis upon linearization by mechanical and electrical design."[3]

However, in spite of the fact that future control system design will tend toward nonlinearization, the complexity of nonlinear differential equations has severely limited the analytical approach to this technique. While some approximate analytical methods have been developed for the analysis of nonlinear systems[3, 4, 5, 6], it is the belief of the authors that the analogue computer is a more convenient and accurate means of overcoming the difficulties encountered in handling nonlinear differential equations. This is particularly true since the art of designing electronic function generators has reached the point where practically all nonlinearities of engineering interest may be accurately and easily simulated.

In summary then, the motivations for a study of this type may be stated as:

(1) The present and potential future utilization of hydraulic servomechanisms.

(2) The growing tendency toward control system optimization by means of nonlinear elements.

With this general introduction, a discussion of hydraulic servo nonlinearities and of the general procedure used for their study in this report follows.

B. Description of Hydraulic Servomechanism Nonlinearities

To familiarize the reader with hydraulic servo nonlinearities, those nonlinearities to be studied in this report will now be discussed in detail.

a. Valve

1. Orifice: The flow rate, Q (expressed in this report by cu. in./sec.), is proportional to the square root of the pressure developed across the orifice*. The pressure developed across the orfice in turn, is dependent upon the load which the fluid is ultimately driving. Therefore, output motion causes load reactive forces, which, when transmitted through the fluid, affect the orifice differential pressure, the square root of which determines the flow rate.

$$Q = Ki\sqrt{P_1} \text{ (assuming } \rho \text{ const.)} \qquad (1\text{-}1)$$

This equation assumes negligible overlap and underlap (see below) in the orifice, and could be plotted as follows (Fig. I-1), where "i" is the current (in ma) entering the solenoid and driving the valve spool.

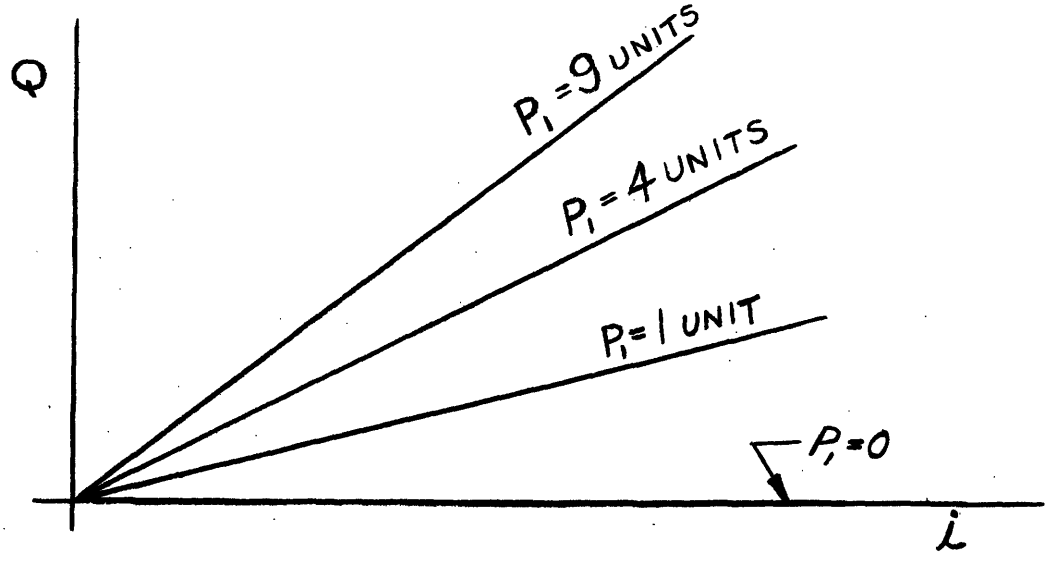

Fig. I-1. Valve flow rate Q, with negligible overlap and underlap; no leakage.

* See Chapter II, Section A.

The square root relationship alone is enough to prohibit rapid analysis by purely analytic means, especially when it is desired to study the effects of parameter variations, such as load inertia, viscous and coulomb damping, and elastic restraint values. Since we have assumed zero overlap and underlap, let us re-examine these two characteristics found in all valves.

2. Overlap and Underlap: If the valve land is of greater or lesser dimension in length than the inlet opening, we have a condition of overlap and underlap, respectively. See Figure I-2(a) and I-2 (b). Valve spool is assumed to be centered.

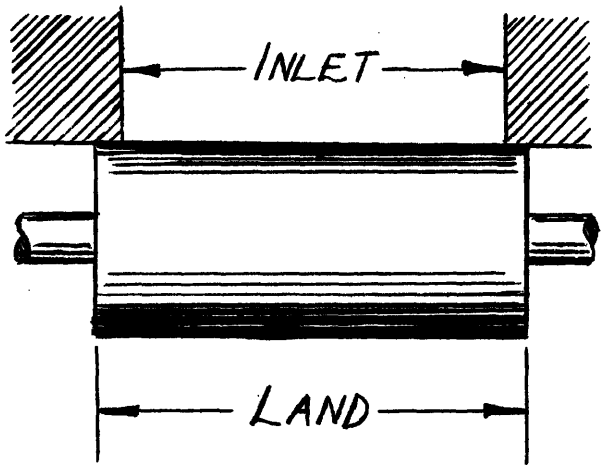

Fig. I-2(a) Overlap condition

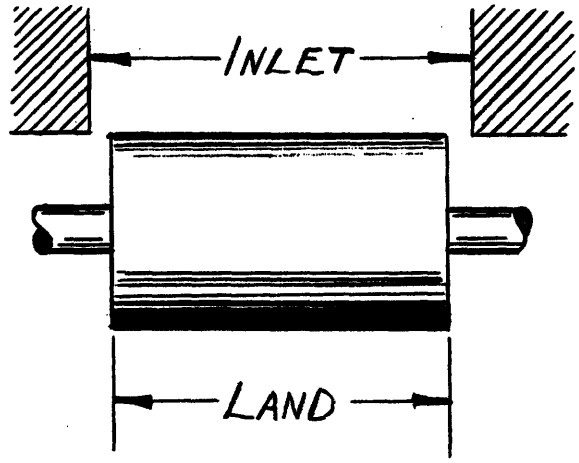

Fig. I-2(b) Underlap condition

The valve flow under these conditions may be shown graphically as in Fig. I-3(a) and I-3(b). Again, it is assumed that an input current is driving the valve spool. Pressure is assumed constant.

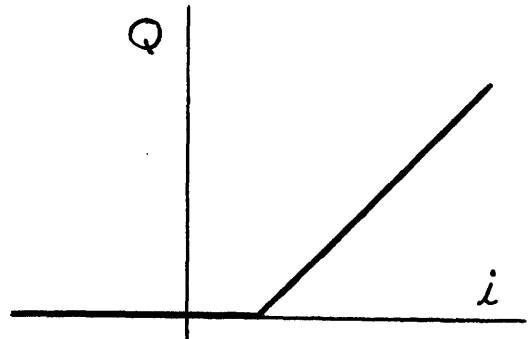

Fig. I-3(a) Flow rate with overlap

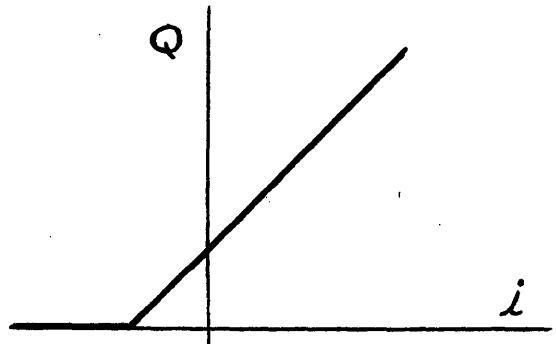

Fig. I-3(b) Flow rate with underlap

3. Leakage: In the above discussion, the leakage was assumed to be negligible; however, in the overlapped valve, the leakage is apparent for both positive and negative values of current. In the underlapped valve, the flow is substantial, even at zero current; consequently, leakage must be considered as that flow which occurs at currents more negative than that required to just close the orifice. In both cases, the principle is basically the same: the leakage flow establishes a minimum flow beneath which the valve will not operate over a finite range of input current. It has been shown that the leakage in a given valve is almost independent of the area of contact between the valve land and valve seat. Fig. I-4(a) and I-4(b) show the net effect of leakage with overlap and underlap respectively.

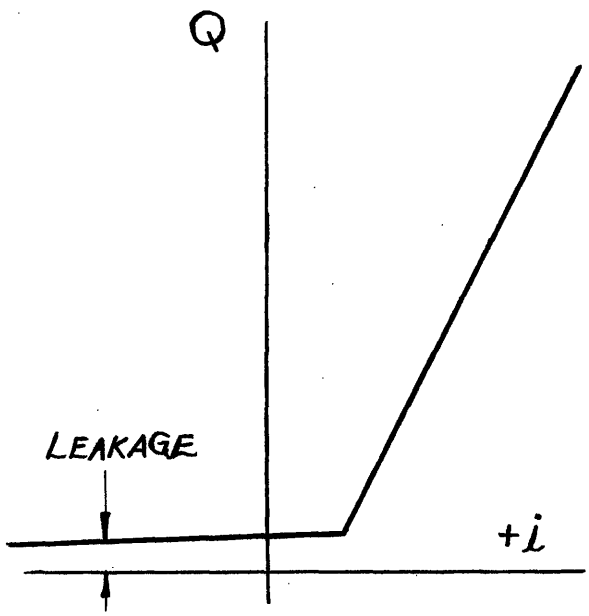

Fig. I-4(a) Leakage in overlapped valve

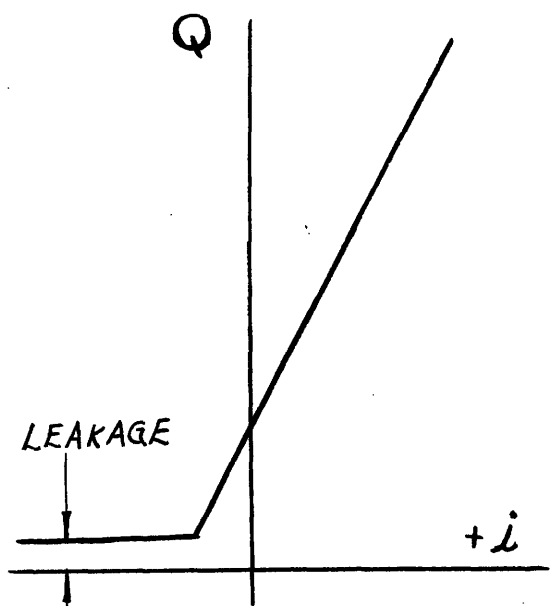

Fig. I-4(b) Leakage in underlapped valve

b. Mechanical System

1. Coulomb Friction. This friction is almost constant in value over the operating velocities encountered in hydraulic systems, and always opposes the motion. It is difficult to treat analytically, since the sign associated with it changes according to the sign of the first derivative of displacement. See Fig. I-5.

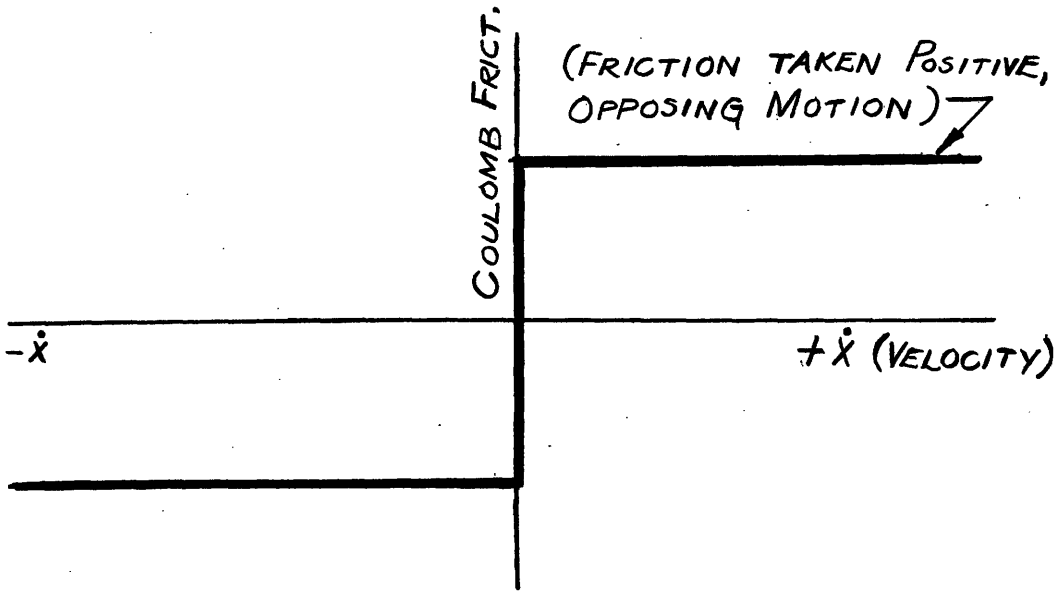

Fig. I-5 Coulomb friction

2. Static Friction. This friction, called "stiction", is the result of breaking the metal "welds" caused by two surfaces being pressed together. It is present only at the start of motion, and may be nearly eliminated by the use of small, superimposed oscillations, often termed "dither". Fig. I-6 illustrates static friction.

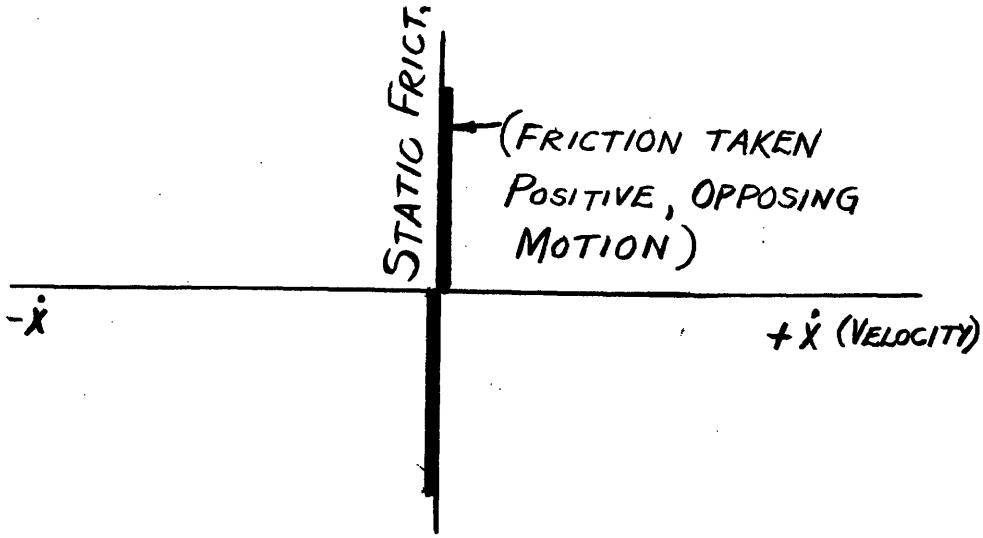

Fig. I-6 Static friction

C. Some Possible Approaches to Nonlinearities

It is obvious that the most accurate way to study a device with nonlinearities is to examine the piece of equipment itself. No other way is exact, and is a compromise between accuracy on the one hand, and speed of investigation and flexibility on the other. One such method is to use an analog computer.

One basic approach with the analog computer is to utilize an element having characteristics very similar to the device itself, but with the added conveniences of small size, flexibility, and low cost. Such an element might be the ordinary vacuum tube. For example, in the study of fluid flow problems, two triodes may be used to form a square law resistor in order to study the relation between viscous friction and fluid velocity.

Another approach would be to assume that the device is linear, and that its relating function may be represented by a simple dynamic term and/ or a constant sensitivity. This is quite satisfactory, if operation is actually to be in a region sufficiently narrow that linearity nearly exists.

Still another way to approximate a nonlinear element would be to build up a piecewise-linear network which, although consisting of short, linear segments, would yield acceptable results. Of course, the accuracy obtained this way depends upon how many segments are used, and may be as high as the requirements of the problem dictate. When diodes are used to form the linear segments of this network, a convenient method of adjusting the network for duplicating the nonlinear element is established by controlling the bias levels of the diodes.

D. General Outline of Procedure

In this investigation we intend to gain familiarity with the system by first treating an ideal case where the valve characteristics are considered linear. The performance equations for this ideal case will be developed. From this beginning, the valve characherisitcs (i.e., nonlinearities) can then be inserted by use of function generators and a multiplier. A limiter will be employed to simulate coulomb damping in the system. "Dither" (a 400 cycle voltage of low amplitude),

will be introduced into the circuit to approximate the conditions actually encountered in practice as closely as possible.

Since our study is principally one of simulation, this report will be largely concerned with the techniques used in intrumenting the system on the analog computer. When the system is completely simulated, we may then observe the changes is system response which result from variation of system parameters.

CHAPTER II

THEORY

A. Fluid Flow Analysis

For the purposes of this report, only the rudimentary equations of fluid flow are required for the complete analysis of the hydraulic servo. The following derivation can be found in any standard fluid mechanics text[7], and is briefly summarized here.

The flow Q equals the area of passage times the velocity of fluid through the given area. But from Bernoulli's theorem,

$$\text{Velocity through an orifice} = \sqrt{2gh} = v \tag{2-1}$$

where h is the pressure head,

and $$h = (\text{pressure})/(\text{density}) = p/\rho \tag{2-2}$$

so $$v = \sqrt{2gp/\rho} \tag{2-3}$$

$$Q = A\sqrt{2gp/\rho} = k\sqrt{p} \tag{2-4}$$

Also we may find the volume of fluid compressed by considering a piston acting upon a confined volume of fluid with a pressure, p.

Then $$V_c = Kp \tag{2-5}$$

where K is the bulk modulus of the fluid defined as

$$\frac{\Delta V}{\Delta p} \quad \frac{in^5}{\#} \quad .$$

Differentiating equation (2-5) we get

$$V_c' = Q_c = Kp' \tag{2-6}$$

B. Analysis of Ideal System

Before proceeding to the analysis of a nonlinear hydraulic servo-

mechanism, the analysis of an ideal hydraulic servo will be carried out in detail (an "ideal" hydraulic servo is here defined as one whose valve characteristic is given by $Q_v = ki_{amp}$); the analysis of the non-linear system will then be regarded as a modification and refinement of the ideal system.

The ideal analysis will be developed as follows. The ideal system is first broken down into a number of convenient components, with each component individually analyzed; each component is then finally coupled together to give the overall ideal system. The overall system with its various components is indicated in Fig. II-1, and the analysis of each component follows. (Note that the servo is assumed to be actuating an aircraft elevator system.) More rigorous development of relating functions for components may be found in the literature[8].

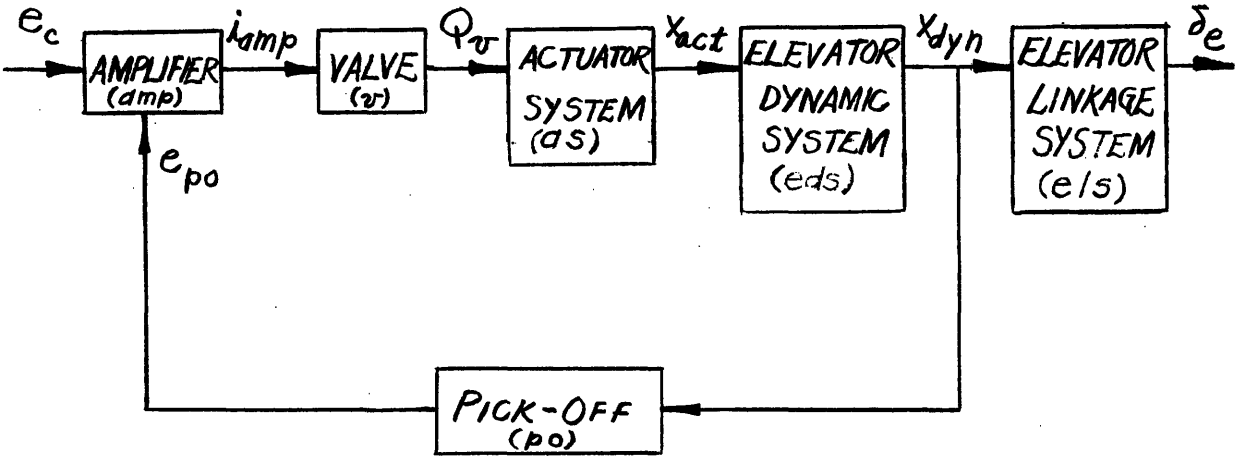

Fig. II-1 Block diagram of ideal hydraulic servo system

a. Analysis of Elevator Dynamic System (eds)

We begin by drawing a schematic diagram of the elevator dynamic system (Fig. II-2).

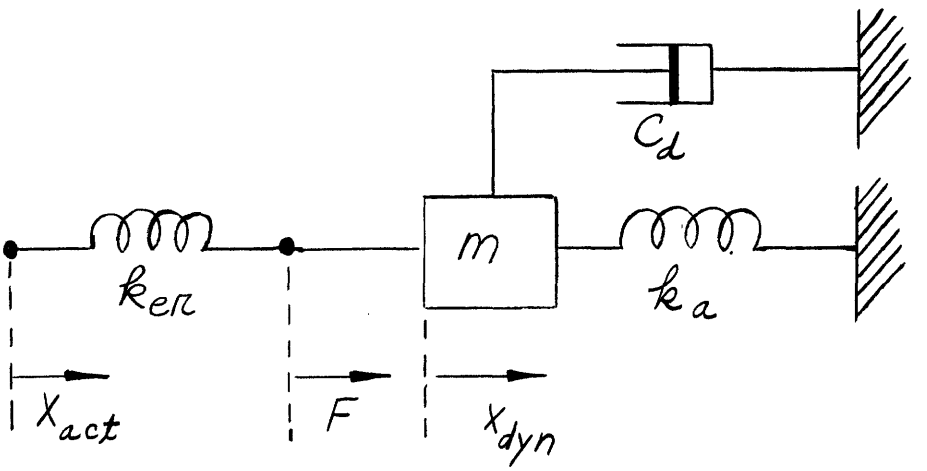

Fig. II-2 Schematic of elevator dynamic system (eds)

In the above diagram, *

m = reflected elevator equivalent mass

C_d = equivalent viscous friction coefficient

k_a = coefficient of aerodynamic restraint

k_{er} = linkage elastic restraint coefficient

From this schematic, the system's differential equation is written as

$$k_{er}(x_{act}-x_{dyn}) = m\ddot{x}_{dyn}+C_d\dot{x}_{dyn}+k_a x_{dyn} \tag{2-7}$$

then

$$\frac{x_{dyn}}{x_{act}} = \frac{k_{er}}{mp^2+C_d p+k_a+k_{er}} = [RF]_{(eds)[x_{act};x_{dyn}]} \tag{2-8}$$

also

$$F = m\ddot{x}_{dyn} + C_d\dot{x}_{dyn} + k_a x_{dyn} \tag{2-9}$$

and

$$\frac{F}{x_{dyn}} = mp^2 + C_d p + k_a = [RF]_{(eds)[x_{dyn};F]} \tag{2-10}$$

* Units for these symbols are given in Appendix A; also see Appendix A for definition of $[RF]$.

From equations (2-8) and (2-10) we obtain the (eds) signal flow diagram (Fig. II-3).

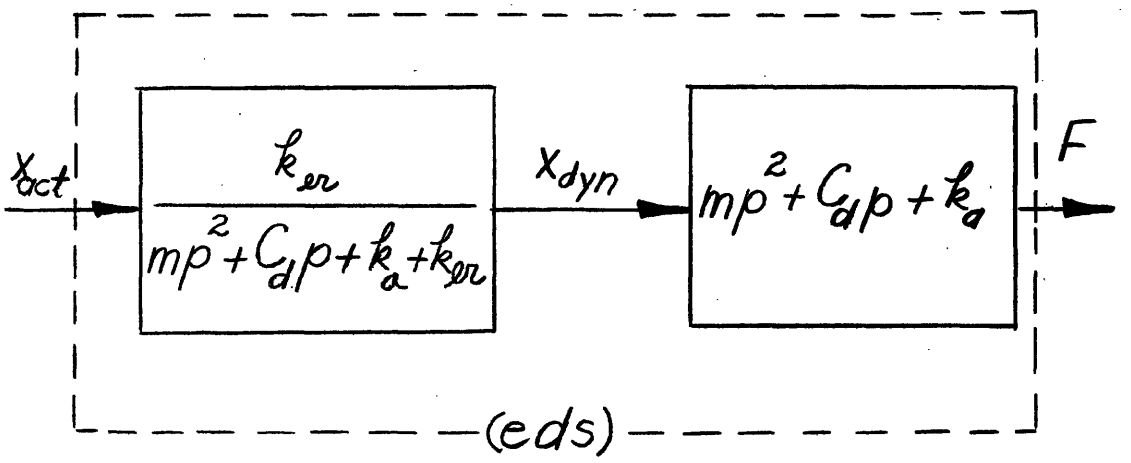

Fig. II-3 Signal flow diagram of (eds)

b. Analysis of Actuator System (as)

Proceeding as before, we indicate the actuator system by a schematic (Fig. II-4).

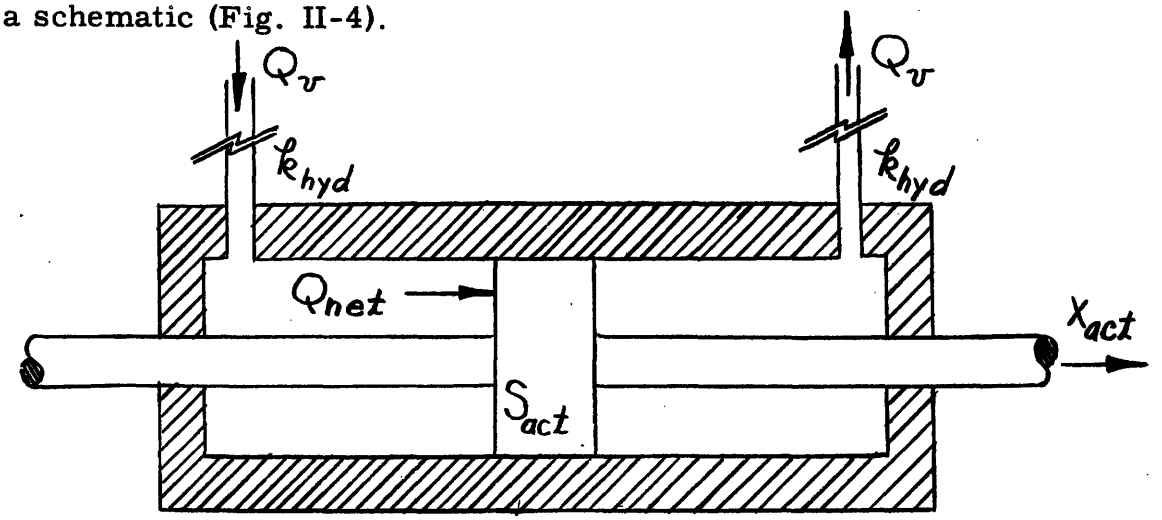

Fig. II-4 Schematic of Actuator System (as)

In the above,

$$S_{act} = \frac{1}{A_{piston}} = \text{actuator sensitivity}$$

k_{hyd} = equivalent elastic restraint coefficient of hydraulic lines.

From equation (2-6),

$$Q_c = \frac{1}{S_{act}\, k_{hyd}} [F]' \tag{2-11}$$

$$\frac{Q_c}{F} = \frac{1}{S_{act}\, k_{hyd}} [p] = [RF]_{(as)}[F; Q_c] \tag{2-12}$$

$$x_{act} = S_{act} \int_0^t Q_{net}\, dt = S_{act} \int_0^t (Q_v - Q_c)\, dt \tag{2-13}$$

$$\therefore \frac{x_{act}}{Q_{net}} = S_{act} \left[\frac{1}{p}\right] = [RF]_{(as)}[Q_{net}; x_{act}] \tag{2-14}$$

From equation (2-14) we obtain the (as) signal flow diagram (Fig. II-5).

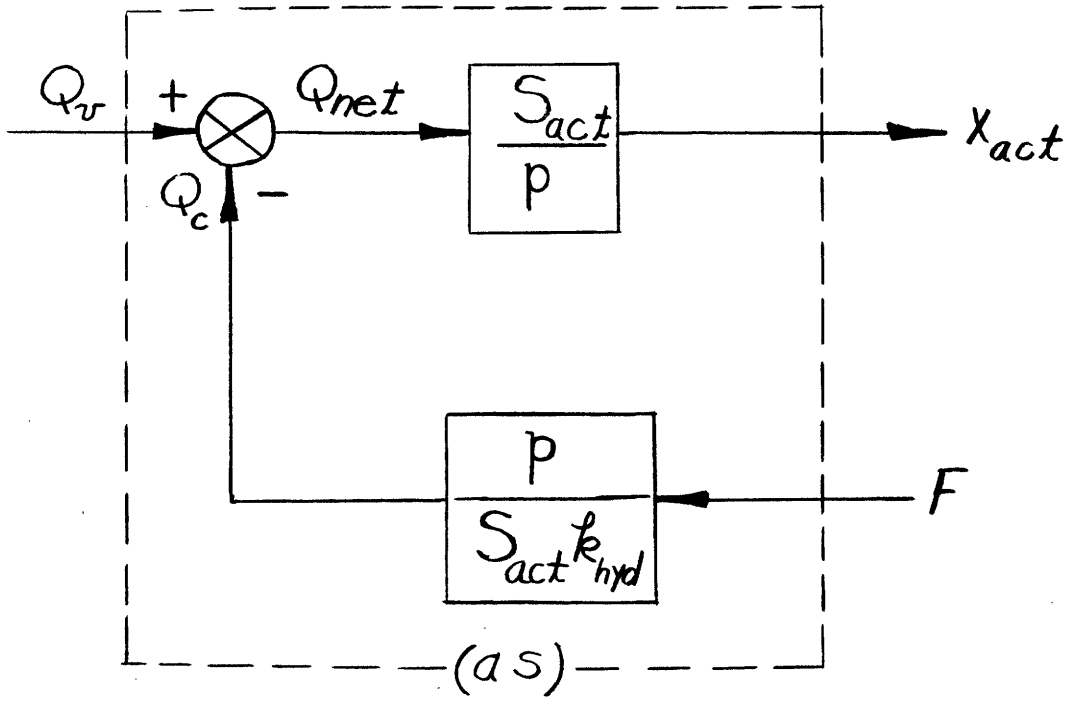

Fig. II-5 Signal flow diagram of (as)

c. Analysis of Valve (v)

In the analysis of the valve, we utilize a schematic diagram (Fig. II-6).

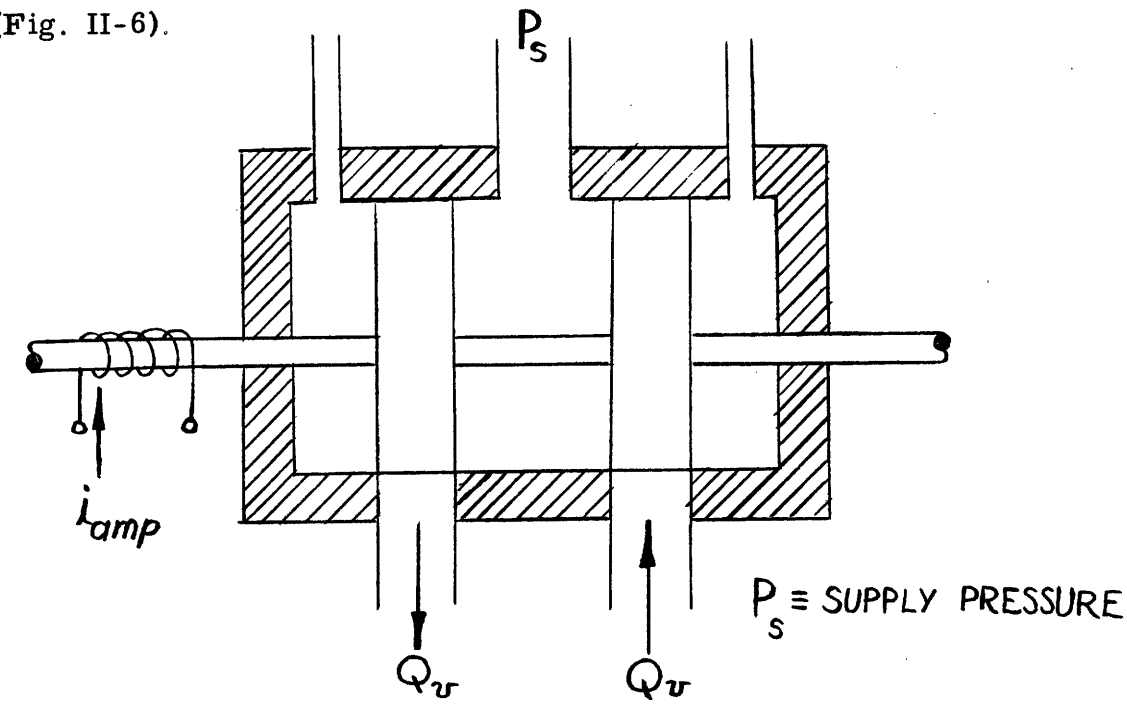

Fig. II-6 Schematic of Valve (v)

Assume

$$Q_v = S_v i_{amp} \tag{2-15}$$

$$\frac{Q_v}{i_{amp}} = S_v = [RF]_{(v)[i;Q]} \tag{2-16}$$

This relationship holds for the ideal case only. Actually, $Q_v = f(i_{amp}, \sqrt{p})$. For the purposes of the ideal analysis only, this inherent nonlinearity is to be temporarily neglected. From equation (2-16) we obtain the (v) signal flow diagram (Fig. II-7).

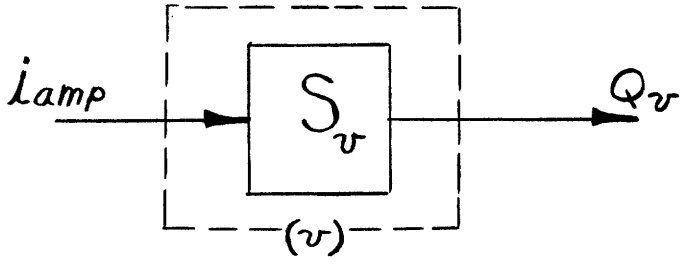

Fig. II-7 Signal flow diagram of (v)

d. Analysis of Amplifier (amp)

The schematic diagram of the amplifier is shown below (Fig. II-8).

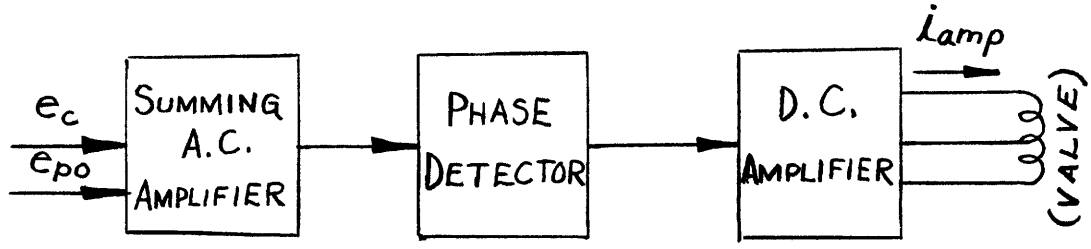

$e_c \equiv$ COMMAND VOLTAGE

$e_{po} \equiv$ PICK-OFF VOLTAGE

Fig. II-8 Schematic of Amplifier (amp)

Assuming negligible phase shift,

$$i_{amp} = S_{amp}(C)\,e = S_{amp}(e_c - e_{po}) \qquad (2\text{-}17)$$

$$\therefore \frac{i_{amp}}{(C)\,e} = S_{amp} = [RF]_{(amp)[e;i]} \qquad (2\text{-}18)$$

From equation (2-18) we obtain the signal flow diagram of the amplifier (Fig. II-9).

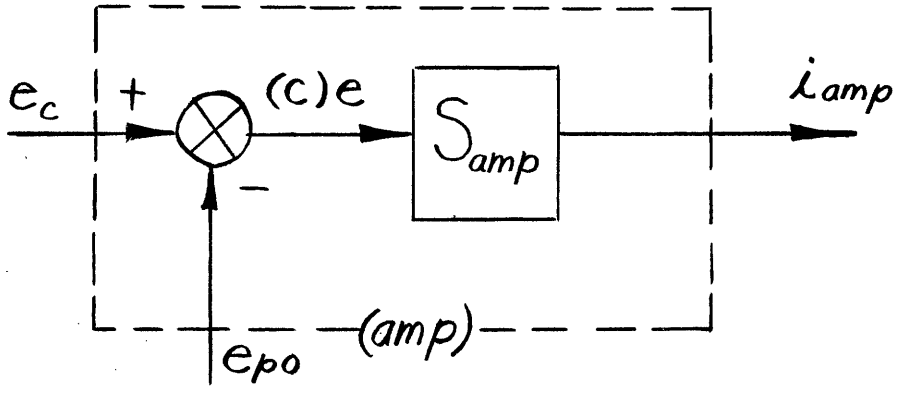

Fig. II-9 Signal flow diagram of (amp)

e. Analysis of Pick-off (po)

This device, commerically called a linearsyn, is represented by the schematic diagram (Fig. II-10).

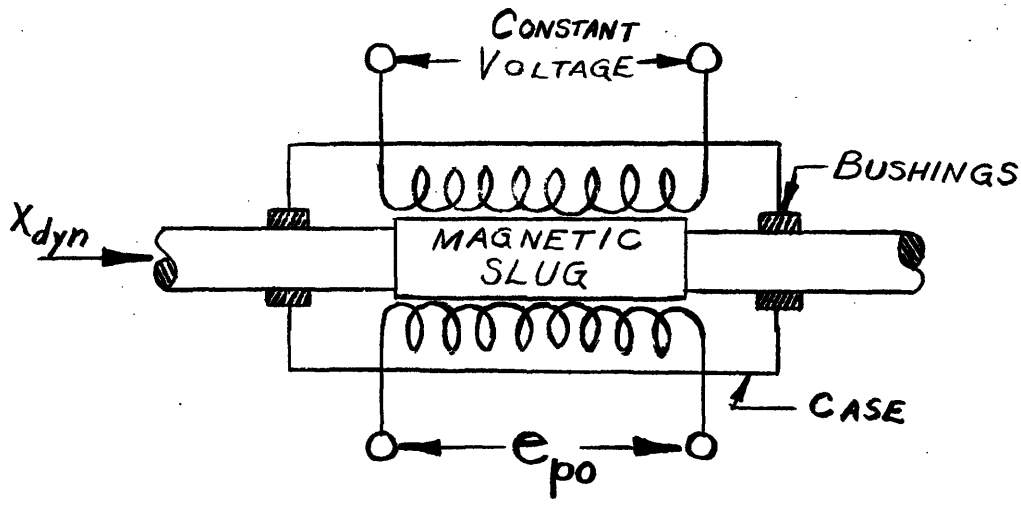

Fig. II-10 Schematic of Pick-off (po)

With negligible dynamics

$$e_{po} = S_{(po)}\, x_{dyn} \tag{2-19}$$

$$\frac{e_{po}}{x_{dyn}} = S_{(po)} = [RF]_{(po)}[x_{dyn}; e_{po}] \tag{2-20}$$

From equation (2-20) we show the signal flow diagram of the pick-off (Fig. II-11).

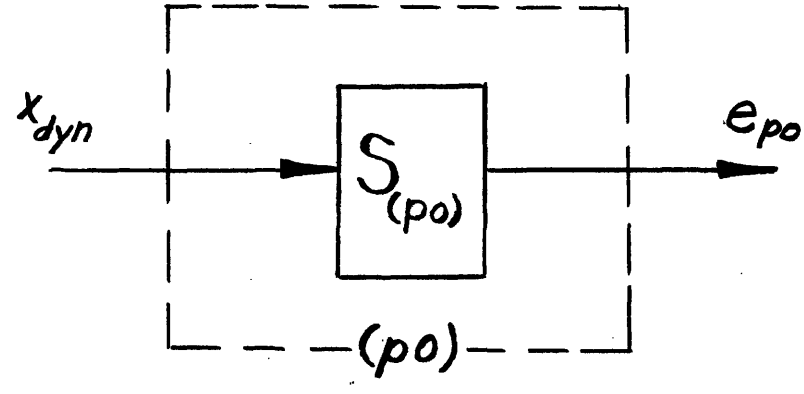

Fig. II-11 Signal flow diagram of (po)

f. Analysis of Elevator Linkage System (els)

This is simply a linkage system for converting the linear motion of the actuator into radial movement of the elevator at the hinge line. The schematic diagram is shown in Fig. II-12.

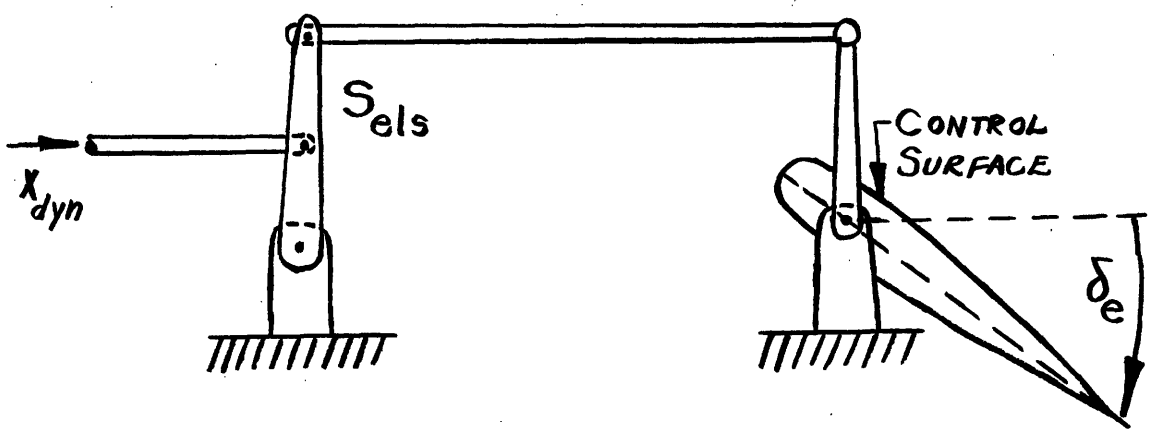

Fig. II-12 Schematic of elevator linkage system (els)

Let $S_{els} \equiv$ Linkage ratio of els

Then
$$\delta_e = S_{els}\, x_{dyn} \tag{2-21}$$

and
$$\frac{\delta_e}{x_{dyn}} = S_{els} \equiv [RF]_{(els)[x;\delta]} \tag{2-22}$$

From equation (2-22) we have the signal flow diagram of (els) (Fig. II-13).

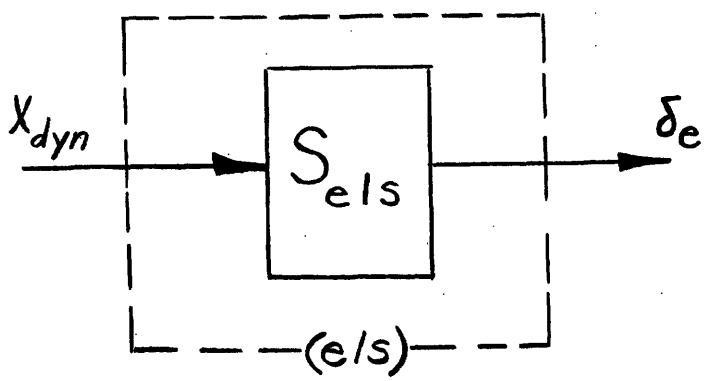

Fig. II-13 Signal flow diagram of (els)

g. Analysis of Entire Hydraulic Servo System (Ideal)

Combining the components of sections a through f, as indicated by Fig. II-1, the overall signal flow diagram is obtained in Fig. II-14. Using the relating functions of each component, as previously derived, the [RF] for the overall ideal hydraulic servo is obtained as follows:

$$[RF]_{(ihs)[e_c;\delta]}$$

$$= \frac{[RF]_{(amp)[e;i]}[RF]_{(v)[i;Q]}[RF]_{(as\text{-}eds)[Q;x]}[RF]_{(els)[x;\delta]}}{1+[RF]_{(amp)[e;i]}[RF]_{(v)[i;Q]}[RF]_{(as\text{-}els)[Q;x]}[RF]_{(els)[x;\delta]}[RF]_{(po)[x;e_{po}]}} \tag{2-23}$$

where:

$$[RF]_{(as\text{-}eds)[Q;x]} = \frac{\frac{S_{act}}{p}\left[\frac{k_{er}}{mp^2+C_dp+k_{er}+k_a}\right]}{1+\frac{S_{act}}{p}\left[\frac{k_{er}}{mp^2+C_dp+k_a+k_{er}}\right]\left[\frac{p}{S_{act}k_{hyd}}\right]\left[mp^2+C_dp+k_a\right]} \tag{2-24}$$

$$= \frac{S_{act}\,k_{er}\,k_{hyd}}{p\left[k_{hyd}(mp^2+C_dp+k_{er}+k_a)+k_{er}(mp^2+C_dp+k_a)\right]} \tag{2-25}$$

$$= \frac{S_{act}\,k_{er}\,k_{hyd}}{p\left[m(k_{hyd}+k_{er})p^2+C_d(k_{hyd}+k_{er})p+k_{hyd}(k_{er}+k_a)+k_{er}k_a\right]} \tag{2-26}$$

Let: $k = k_{hyd} + k_{er}$ (2-27)

Then:

$$[RF]_{(ihs)[e_c;\delta]} =$$

$$\frac{\dfrac{S_{amp}S_vS_{els}S_{act}k_{er}k_{hyd}}{p\left[mkp^2+C_dkp+k_{hyd}(k_{er}+k_a)+k_{er}k_a\right]}}{1+\dfrac{S_{po}S_{amp}S_vS_{act}k_{er}k_{hyd}}{p\left[mkp^2+C_dkp+k_{hyd}(k_{er}+k_a)+k_{er}k_a\right]}} \qquad (2\text{-}28)$$

$$= \frac{S_{amp}\,S_v\,S_{els}\,S_{act}\,k_{er}\,k_{hyd}}{p\left[mkp^2+C_dkp+k_{hyd}(k_{er}+k_a)+k_{er}k_a\right]+S_{po}S_{amp}S_vS_{act}k_{er}k_{hyd}} \qquad (2\text{-}29)$$

$$[RF]_{(ihs)[e_c;\delta]} =$$

$$\frac{S_{amp}\,S_v\,S_{els}\,S_{act}\,k_{er}\,k_{hyd}}{mkp^3+C_dkp^2+(k_{hyd}k_{er}+k\,k_a)p+S_{po}S_{amp}S_vS_{act}k_{er}k_{hyd}}$$

= Relating Function of ideal hydraulic servo, for command voltage in, elevator deflection out

(2-30)

For the simulation of the above equation, the reader is referred to Chapter IV.

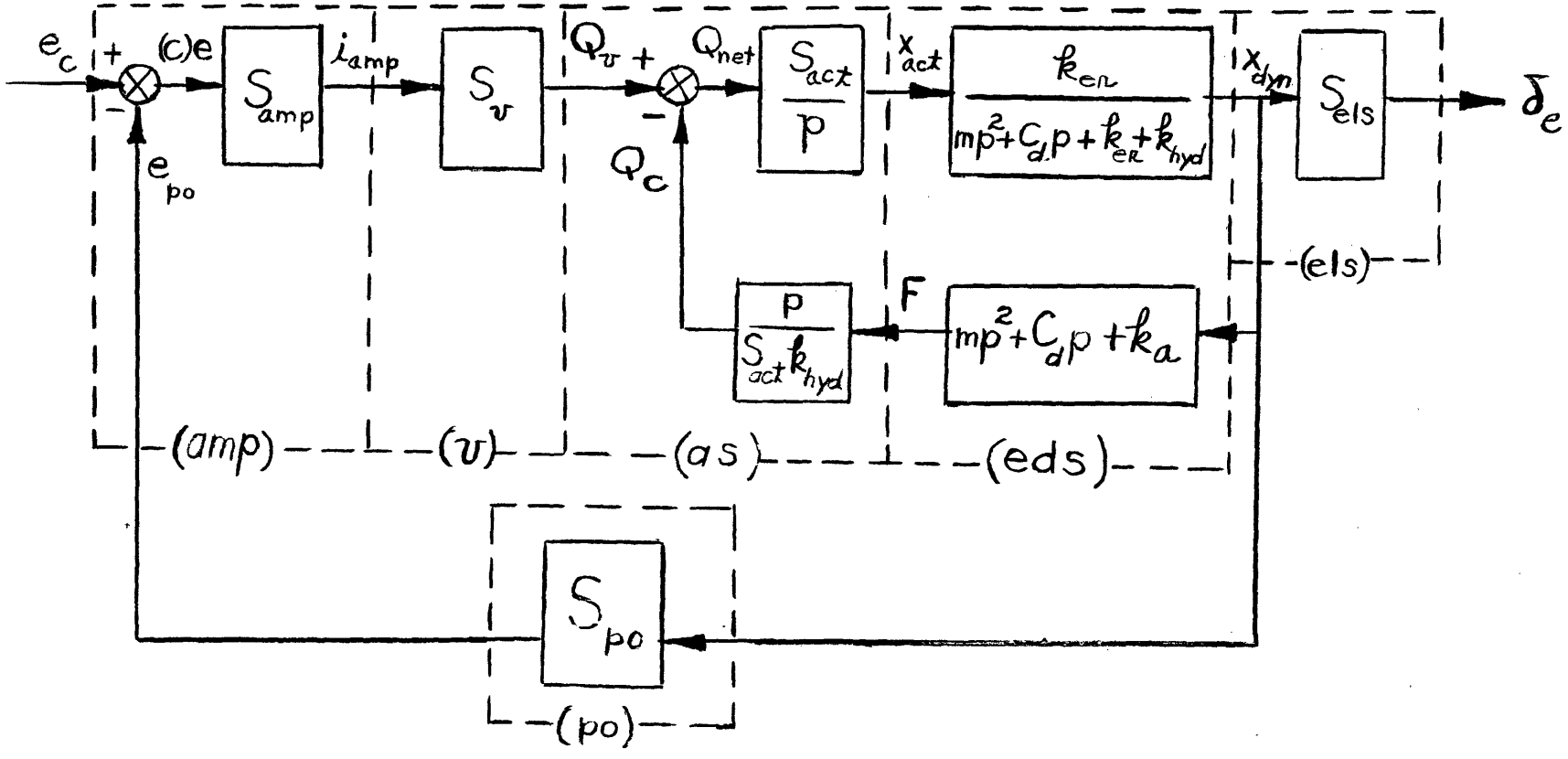

Fig. II-14 Overall signal flow diagram of ideal hydraulic servomechanism system (ihs).

C. Analysis of the Nonlinear Hydraulic Servomechanism

Starting from the overall system block diagram (Fig. II-15), each part is analyzed in turn.

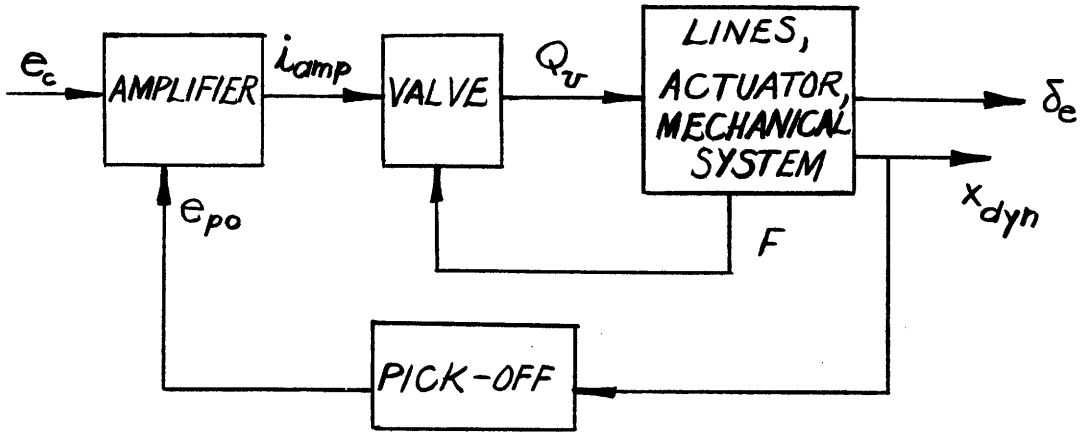

Fig. II-15 Block Diagram of Nonlinear Hydraulic Servo.

a. Amplifier.

For our purposes, this is simply a sensitivity, with no phase angle (as in ideal analysis).

b. Valve.

For convenience, we assume balanced loads and balanced valves, and study only one half of the valve's hydraulic circuit. Thus, the valve spool and cylinder may be "cut" in two, as shown in Fig. II-16.

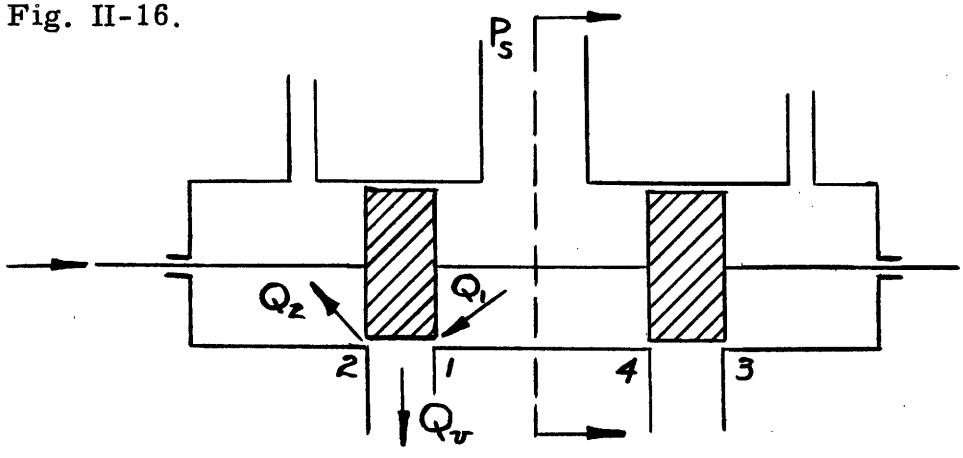

Fig. II-16 Section of Valve

Now, $Q_v = Q_1 - Q_2$ and furthermore, Q_1 and Q_2 are dependent upon the pressures across the orifices through which they flow. That is,

$$Q_1 = ki\sqrt{\Delta P_1} \qquad (2\text{-}31)$$

and likewise, $$Q_2 = ki\sqrt{\Delta P_2} \qquad (2\text{-}32)$$

where k is a constant, and i is current driving the solenoid.

These square roots are difficult to set up on an analog computer, so a means of approximation will be used. Remembering the balanced conditions of operation, we may draw an equivalent bridge circuit (Fig. II-17).

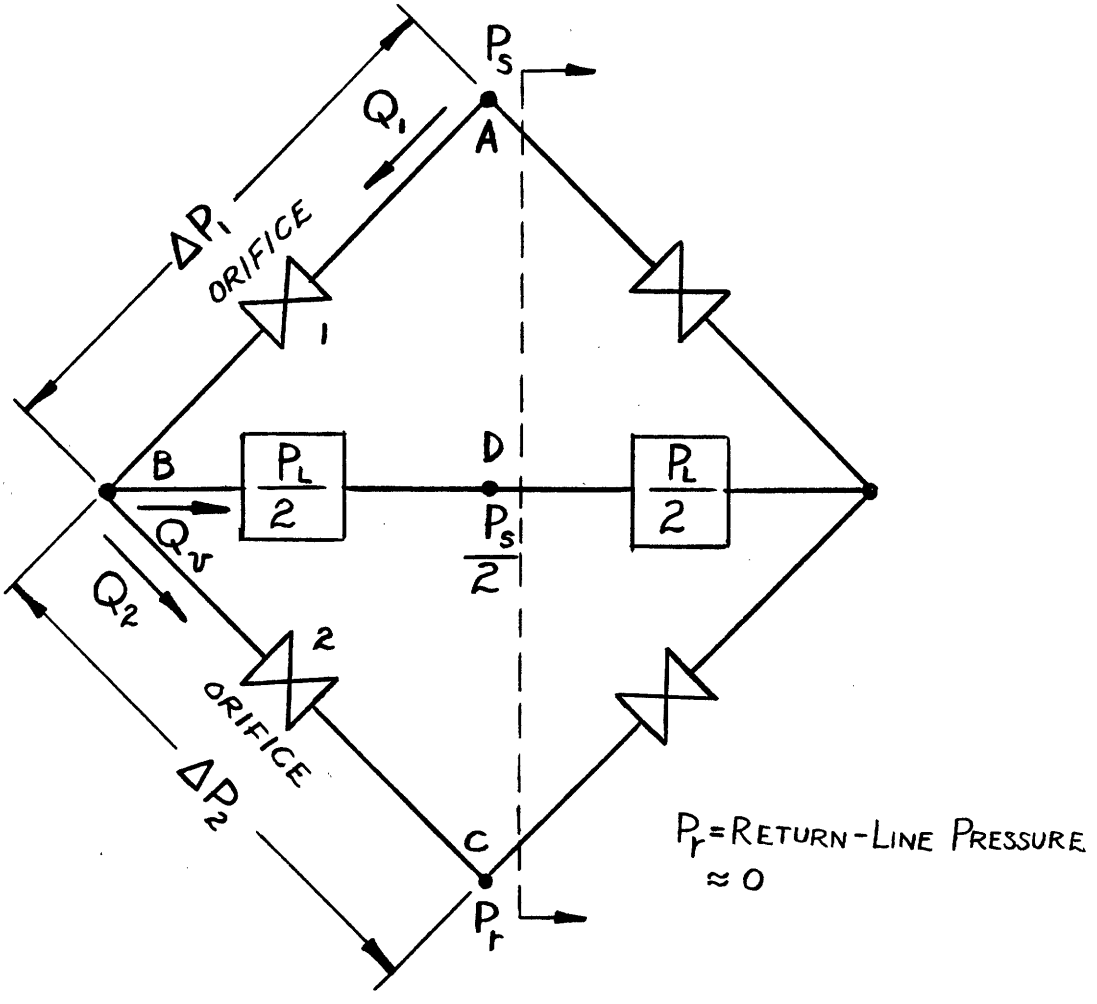

Fig. II-17 Valve Equivalent Bridge Circuit

The point D is at a pressure of $P_s/2$, where P_s is the supply pressure, assuming $P_r \approx 0$. Dropping the delta prefix on P_1 and P_2 , we may express them in terms of P_s and P_L , where P_L is the pressure exerted by the load due to interfering moments and load dynamics.

$$\Delta P_1 = P_1 = P_s - (P_s+P_L)/2 = (P_s-P_L)/2 \tag{2-33}$$

$$\Delta P_2 = P_2 = P_s - P_1 = (P_s+P_L)/2 \tag{2-34}$$

so, $$Q_1 = k_1 i\sqrt{(P_s-P_L)/2} \tag{2-35}$$

and, $$Q_2 = k_2 i\sqrt{(P_s+P_L)/2} \tag{2-36}$$

Approximating,

$$Q_1 = k_1 i\sqrt{P_s/2}\left[1-\frac{1}{2}\frac{P_L}{P_s}\right] \tag{2-37}$$

$$Q_2 = k_2 i\sqrt{P_s/2}\left[1-\frac{1}{2}\frac{P_L}{P_s}\right] \tag{2-38}$$

In general, $Q_{\text{no load}} = ki\sqrt{P_s/2}$, since $P_L = 0$ (2-39)

Therefore, if we have the curves for Q_1 and Q_2 at no load, we may obtain the curves for load conditions as follows:

$$Q_1 = Q_{1 \text{ no load}}\left[1-\frac{1}{2}\frac{P_L}{P_s}\right] \tag{2-40}$$

$$Q_2 = Q_{2 \text{ no load}}\left[1+\frac{1}{2}\frac{P_L}{P_s}\right] \tag{2-41}$$

Now,

$$Q_v = Q_1 - Q_2 \tag{2-42}$$

$$= Q_{1\,n.l.} - Q_{1\,n.l.}\left(\frac{1}{2}\frac{P_L}{P_s}\right) - Q_{2\,n.l.} - Q_{2n.l.}\left(\frac{1}{2}\frac{P_L}{P_s}\right) \tag{2-43}$$

$$Q_v = \left[Q_{1n.l.} - Q_{2n.l.}\right] - \frac{1}{2}\frac{P_L}{P_s}\left[Q_{1n.l.} + Q_{2n.l.}\right] \tag{2-44}$$

This may be obtained easily on the analog computer, as seen in Chapter IV.

c. Lines, Actuator, Mechanical System.

For convenience, we shall call this the linkage system, since it connects the valve output to the elevator by means of fluid flow and mechanical linkages.

The relating function for this system will be written in terms of V_v in, and x_{dyn} out, for ease in instrumenting it later on the analog set-up.

$$[RF]_{(as-eds)} = [RF]_{linkage}\,[V_v\,;\,x_{dyn}] \tag{2-45}$$

$$= \frac{S_{act}\,k_{er}\,k_{hyd}}{m(k_{hyd}+k_{er})p^2+C_d(k_{hyd}+k_{er})p+k_a(k_{hyd}+k_{er})+k_{er}k_{hyd}} \tag{2-46}$$

(For the derivation of equation (2-46), see section II-B. Also see section II-B for obtaining F_{dyn}.)

Coulomb friction will be added when the actual computer diagrams are considered (Chapter IV), since it is more conveniently handled then than it is in equation form.

d. Pick-off .

This, as in the case of the amplifier, is simply a sensitivity, with phase angle considered zero.

For simulation of the above, see Chapter IV.

CHAPTER III

APPARATUS

It may be helpful to describe briefly the equipment used in the simulation carried out in this report. (All equipment to be discussed in detail was designed and developed by the MIT Instrumentation Laboratory, Analogue Computation Group.) The main piece of apparatus, of course, is the analog computer itself, called the General Purpose Simulator (GPS). Other items used include a master generator, two function generators, an electronic multiplier, a second order unit, and assorted smaller units such as an oscilloscope, two limiters, and signal generators.

A. General Purpose Simulator

The simulator used in obtaining data for this report contains 7 integrators, 10 summing amplifiers, 21 potentiometers, and a number of other features that enable one to simulate and solve differential equations of order as high as seven. Two of the aforementioned potentiometers consist of two units ganged together, so that two parameters may be varied simultaneously at identical values. This particular feature was of great help in the present study, since the assumption of balanced values implies that the lap and leakage of one orifice equals the lap and leakage of the other.

The integrators have time constants which may be set as high as 3000, so that problems may be observed in real time units, as well as in "slowed down" time.

B. Master Generator

This generator supplies a step (or impulse, if needed) voltage

output (100 volts), and a calibrating line which may be displayed simultaneously with the problem on the oscilloscope, so that quantity as well as quality of system response may be studied conveniently. Another feature of this generator is that it supplies a time reference. This is obtained by connecting the generator's time dot intensity output to the "z" input of the scope; the scope's response trace (and the calibrating line) is then illuminated at periodic time intervals (.02 seconds in this study), so that time of response, etc., may be readily determined without reference to inaccurate grid overlays.

C. Function Generators

These were simply small electronic units designed for the purpose of duplicating the sensitivity curve of any piece of equipment (in particular, for duplicating hydraulic valve nonlinearities). Bias levels may be set so that the operating level of the diodes within the function generators are such that desired slopes and intercepts are obtained.

D. Electronic Multiplier

This multiplier accurately multiplies two arbitrary functions, and will also supply the sum and difference of the input quantities. The multiplier was very useful in simulating the effect of pressure feedback on the valve characteristics.

E. Second Order Unit

This unit supplies a second order lag adjustable to any desired damping ratio and natural frequency. Its use obviates the effort and complexity of wiring two additional integrators.

F. Other Equipment

No mention will be made of the other small units used in the set-up, since their contribution to the overall problem is not important.

For a view of the set-up used, see Fig. III-1. The GPS is seen in the center. To the left is the electronic multiplier and to the right, placed above the master generator, are the oscilloscope and second order unit.

For more detailed information regarding this equipment the reader is referred to the bibliography[9].

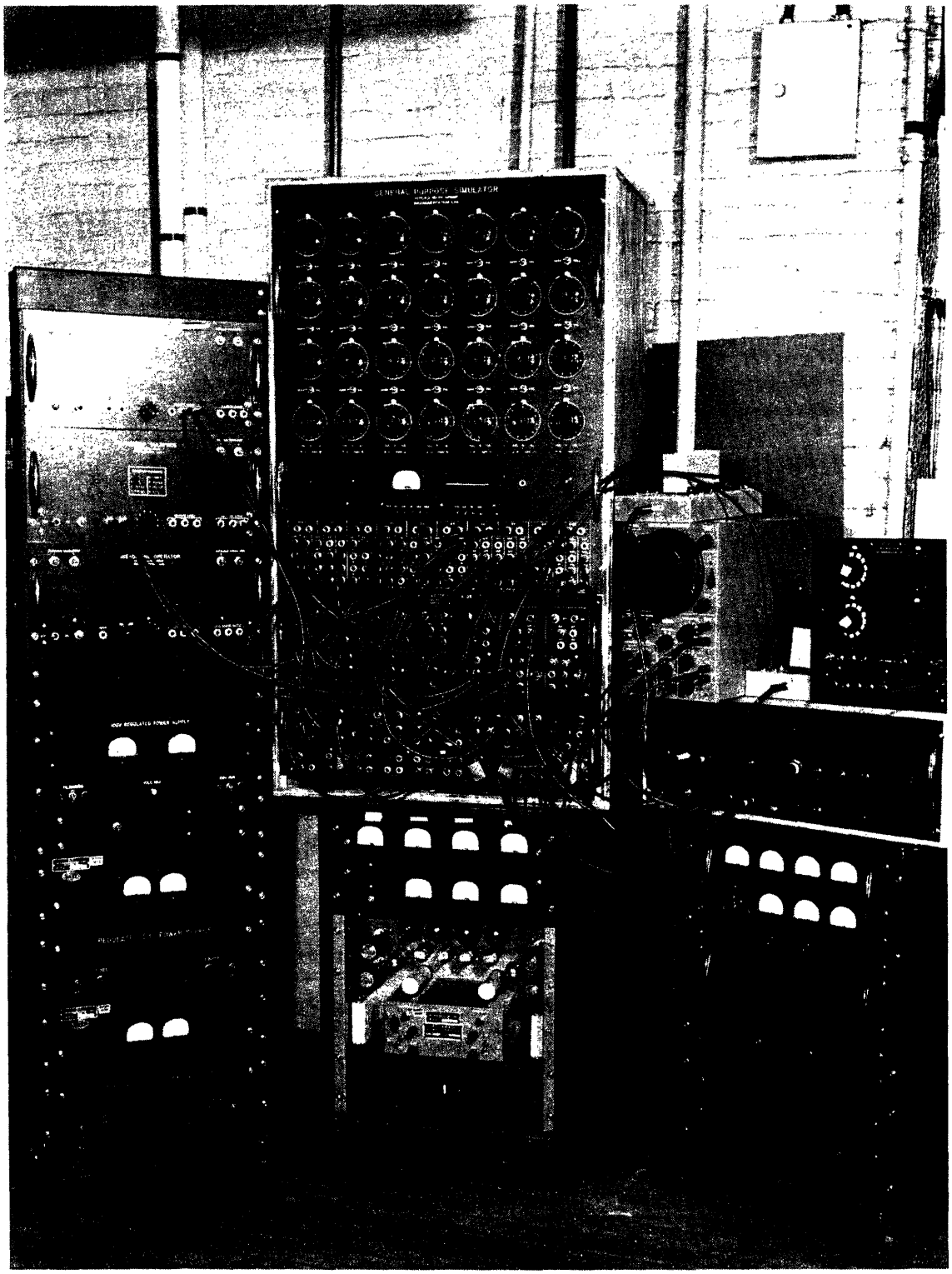

Fig. III -1 View of simulator apparatus

CHAPTER IV

SIMULATION

A. Development of Numerical Constants

a. The actuator sensitivity is equal to the reciprocal of the area of the actuator piston, and can be defined as the derivative of the ratio of output displacement, $x_{act,}$ to fluid flow to the valve, Q_{act} .

Or

$$S_{act} = p\left[\frac{x_{act}}{Q_{act}}\right] = 1.81 \text{ in}^{-2} \text{ (measured value).} \qquad (4\text{-}1)$$

b. The elevator linkage system sensitivity is angular elevator displacement per unit linear actuator displacement:

$$S_{els} = \frac{\delta_e}{x_{act}} = 2.81 \text{ deg/in} = 0.49 \text{ rad/in} \qquad (4\text{-}2)$$

c. The actual elevator deflection would be $(S_{els}\, x_{act})$ minus the loss due to system compliance which is a function of the force on the actuator. Therefore:

$$\delta_e = S_{els}\, x_{act} - S_{els}\, S_{er} A_{act}\, P_L \qquad (4\text{-}3)$$

where S_{er} is the mechanical compliance of the linkage between actuator and elevator, and P_L is the pressure drop across the actuator. Substituting Eq. (4-1) into Eq. (4-3), we have:

$$\delta_e = S_{els}\, S_{act}\left[\frac{Q_{net}}{p}\right] - S_{els}\, S_{er} A_{act}\, P_L \qquad (4\text{-}4)$$

The flow to the actuator is the flow out of the valve less the flow loss due to compressibility of the fluid. In the static case where there is no flow from the valve:

$$Q_{net} = Q_c = S_{hyd}\ p\left[P_L\right] \tag{4-5}$$

where S_{hyd} is defined as :

$$S_{hyd} = \frac{\Delta V}{\Delta P} in^5/\# \tag{4-6}$$

Substitution of Eq. (4-5) into Eq. (4-4) gives:

$$\delta_e = S_{els}\, S_{act}\, S_{hyd}\, P_L + S_{els}\, S_{er}\, A_{act}\, P_L$$

$$= P_L\, S_{els}\, (S_{act}\, S_{hyd} + S_{er}\, A_{act}) \tag{4-7}$$

With the piston locked, the actuator, connecting rods, and elevator can be assumed to be a second order system with characteristic equation as follows.

$$(Ip^2 + c_d\, p + k)\, \delta_e = 0$$

$$\text{or} \quad \frac{p^2}{\frac{k}{I}} + \frac{p}{\frac{k}{c_d}} + 1 = \frac{p^2}{\omega_n^2} + \frac{2\zeta}{\omega_n} p + 1 = 0 \tag{4-8}$$

$$\text{where } \omega_n = \sqrt{\frac{k}{I}} \tag{4-9}$$

k can be defined as the torque at the elevator hinge line due to an applied elevator deflection, δ_e, with piston locked:

$$k = \frac{M_{eh}}{\delta_e} \tag{4-10}$$

The moment at the hinge line can be described by Fig. IV-1.

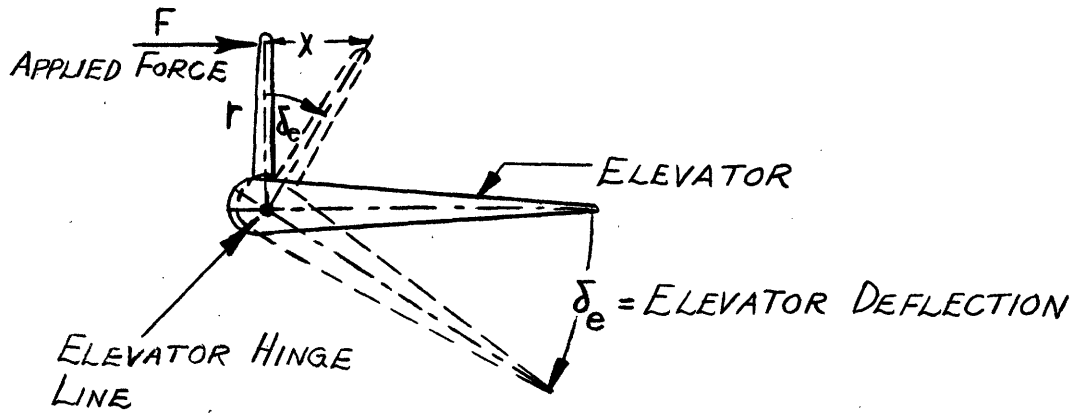

$$M_{eh} = F_r = A_{act} P_L r$$

$$\tan \delta_e = \frac{x}{r} \approx \delta_e \quad (\delta_e \text{ is small for locked piston})$$

$$S_{els} = \frac{\delta_e}{x} = \frac{x}{r}\left(\frac{1}{x}\right) = \frac{1}{r}$$

$$\therefore M_{eh} = \frac{A_{act} P_L}{S_{els}}$$

Fig. IV-1 Schematic of Elevator and Hinge Line

Substituting the results of Fig. IV-1 and equation (4-7) into equation (4-10), we have:

$$k = \frac{A_{act} P_L}{S_{els} \delta_e} = \frac{A_{act} P_L}{S_{els}\left[P\, S_{els} (S_{act} S_{hyd} + S_{er} A_{act})\right]} \qquad (4\text{-}11)$$

or,
$$k = \frac{A_{act}}{S_{els}^2}\left[\frac{1}{S_{act} S_{hyd} + S_{er} A_{act}}\right] \qquad (4\text{-}12)$$

then from equations (4-9) and (4-12)

$$\omega_n = \sqrt{\frac{A_{act}}{I S_{els}^2}\left(\frac{1}{S_{act} S_{hyd} + S_{er} A_{act}}\right)} \qquad (4\text{-}13)$$

or, since $S_{act} = \frac{1}{A_{act}}$,

$$\omega_n = \sqrt{\frac{1}{I\, S_{els}^2\, (S_{act}^2\, S_{hyd} + S_{er}}} \qquad (4\text{-}14)$$

With the piston locked, a step displacement was applied to the elevator and the vibration of the elevator about its hinge line (with near zero damping) was recorded as 30 cps. With piston unlocked, this vibration was recorded as 15cps. The first condition would correspond to $S_{hyd} = 0$.

From equation (4-14) we have:

$$S_{act}^2\, S_{hyd} + S_{er} = \frac{1}{\omega_n^2\, I\, S_{els}^2} \qquad (4\text{-}15)$$

$I_{elev.}$ was known to be $1100\#\ in^2 = 2.85\#in\ sec^2$

so

$$S_{act}^2\, S_{hyd} + S_{er} = \frac{1}{\omega_n^2\, (2.85)(0.49)^2} = \frac{1.46}{\omega_n^2}\ \frac{in}{\#} \qquad (4\text{-}16)$$

With the actuator locked (i.e., $S_{hyd} = 0$), $\omega_n = 30$cps and:

$$S_{er} = \frac{1.46}{(30 \times 2\pi)^2} = 4.12 \times 10^{-5}\ in/\# \qquad (4\text{-}17)$$

or

$$k_{er} = \frac{1}{S_{er}} = 2.43 \times 10^4\ \#/in \qquad (4\text{-}18)$$

With the actuator unlocked, $\omega_n = 15$cps and equation (4-16) becomes:

$$S_{act}^2\, S_{hyd} + 4.12 \times 10^{-5} = \frac{1.46}{(15 \times 2\pi)^2} \qquad (4\text{-}19)$$

Since $S_{act} = 1.81\ in^{-2}$ (see below)

$$S_{hyd} = \left[\frac{1.46}{(15 \times 2\pi)^2} - 4.12 \times 10^{-5}\right]\left[\frac{1}{1.81}\right]^2 = 3.77 \times 10^{-5}\ \frac{in^5}{\#} \qquad (4\text{-}20)$$

and

$$k_{hyd} = \frac{1}{S_{hyd}}\left(\frac{1}{S_{act}^2}\right) = \frac{1}{3.77 \times 10^{-5}} \times \frac{1}{1.81^2} = 0.8 \times 10^4 \ \#/\text{in} \quad (4\text{-}21)$$

The following constants were obtained by direct measurement:

$$S_{amp} = 20 \text{ ma/volt}$$

$$S_{act} = 1.81 \text{ in}^{-2}$$

$$S_{po} = 3.93 \text{ volts/in}$$

$$S_{els} = .49 \text{ rad/in}$$

$$S_v = .587 \frac{\text{in}^3/\text{sec}}{\text{ma.}}$$

B. Simulation of Ideal Hydraulic Servo

The simulation of the ideal $[RF]_{(ihs)[e_c;\delta_e]}$ developed in Chapter II serves as an excellent illustration of the technique employed in simulating higher order differential equations. From Chapter II, Section B, the above relating function is:

$$[RF]_{(ihs)[e_c;\delta]} = \frac{S_{amp} S_v S_{act} S_{els} k_{er} k_{hyd}}{mkp^3 + C_d k p^2 + (k_{hyd} k_{er} + k k_a) p + S_{po} S_{amp} S_v S_{act} k_{er} k_{hyd}} \quad (4\text{-}22)$$

Using the values developed in Section A of this chapter, the various coefficients above are calculated as follows (C_d and k_a are to be retained as variable parameters):

$$S_{amp} S_v S_{els} S_{act} k_{er} k_{hyd} =$$

$$\left(20\frac{\text{ma}}{\text{v}}\right)\left(0.587\frac{\text{in}^3}{\text{sec.ma}}\right)\left(0.49\frac{\text{rad}}{\text{in}}\right)\left(1.81\text{in}^{-2}\right)\left(2.52\text{x}10^4\frac{\#}{\text{in}}\right)\left(0.837\text{x}10^4\frac{\#}{\text{in}}\right)$$

$$= 22 \times 10^8 \ \#^2/\text{v-sec-in}^2 \quad (4\text{-}23)$$

$S_{amp}S_vS_{act}S_{po}\,k_{er}\,k_{hyd} =$

$$(20\,\frac{ma}{v})(0.587\,\frac{in^3}{sec.\,ma})(3.93\,\frac{v}{in})(1.81\,in^{-2})(2.52\times10^4\,\frac{\#}{in})(0.837\times10^4\,\frac{\#}{in})$$

$$= 176\times10^8\,\frac{\#^2}{sec - in^2} \qquad (4\text{-}24)$$

$$k=k_{er}+k_{hyd}=2.52\times10^4\,\frac{\#}{in}+0.837\times10^4\,\frac{\#}{in} = 3.357\times10^4\,\frac{\#}{in} \qquad (4\text{-}25)$$

$$k_{hyd}k_{er}+k\,k_a = (2.52\times10^4\,\frac{\#}{in})(0.837\times10^4\,\frac{\#}{in})+(3.357\times10^4)\,k_a$$

$$= 2.11\times10^8 + 3.357\times10^4\,k_a \qquad (4\text{-}26)$$

$$mk = (0.684\,\frac{\#sec^2}{in})(3.357\times10^4\,\frac{\#}{in}) = 2.29\times10^4\,\frac{\#^2sec^2}{in^2} \qquad (4\text{-}27)$$

$$C_dk = 3.357\times10^4\,C_d\,\frac{\#^2sec}{in^2} \qquad (4\text{-}28)$$

Thus,

$[RF]_{(ihs)[e_c;\,\delta]} =$

$$\frac{22\times10^8}{[2.29\times10^4p^3+3.357\times10^4C_dp^2+(2.11\times10^8+3.357\times10^4k_a)p+176\times10^8]}$$

$$= \frac{22\times10^4}{2.29p^3+3.357C_dp^2+(2.11\times10^4+3.357k_a)p+176\times10^4},\ v^{-1} \qquad (4\text{-}29)$$

$$S_{(ihs)[e_c;\,\delta]} = \frac{22\times10^4}{176\times10^4} = 0.125\,\frac{rad}{v} \qquad (4\text{-}30)$$

Check:

$$S_{(ihs)[e_c;\delta]} = \frac{S_{els}}{S_{po}} = \frac{0.49\ \frac{rad}{in}}{3.93\ \frac{v}{in}} = 0.125\ \frac{rad}{v} \qquad (4\text{-}31)$$

From the above:

$$2.29\frac{d^3\delta}{dt^3} + 3.357C_d\frac{d^2\delta}{dt^2} + (2.11\times10^4 + 3.357k_a)\frac{d\delta}{dt} + 176\times10^4\delta = 22\times10^4 e_c \qquad (4\text{-}32)$$

So that

$$2.29p^3\delta = 22\times10^4 e_c - 3.357C_d p^2\delta - (2.11\times10^4 + 3.357k_a)p\delta - 176\times10^4\delta \qquad (4\text{-}33)$$

We can now draw a tentative simulator schematic, Fig. IV-2.

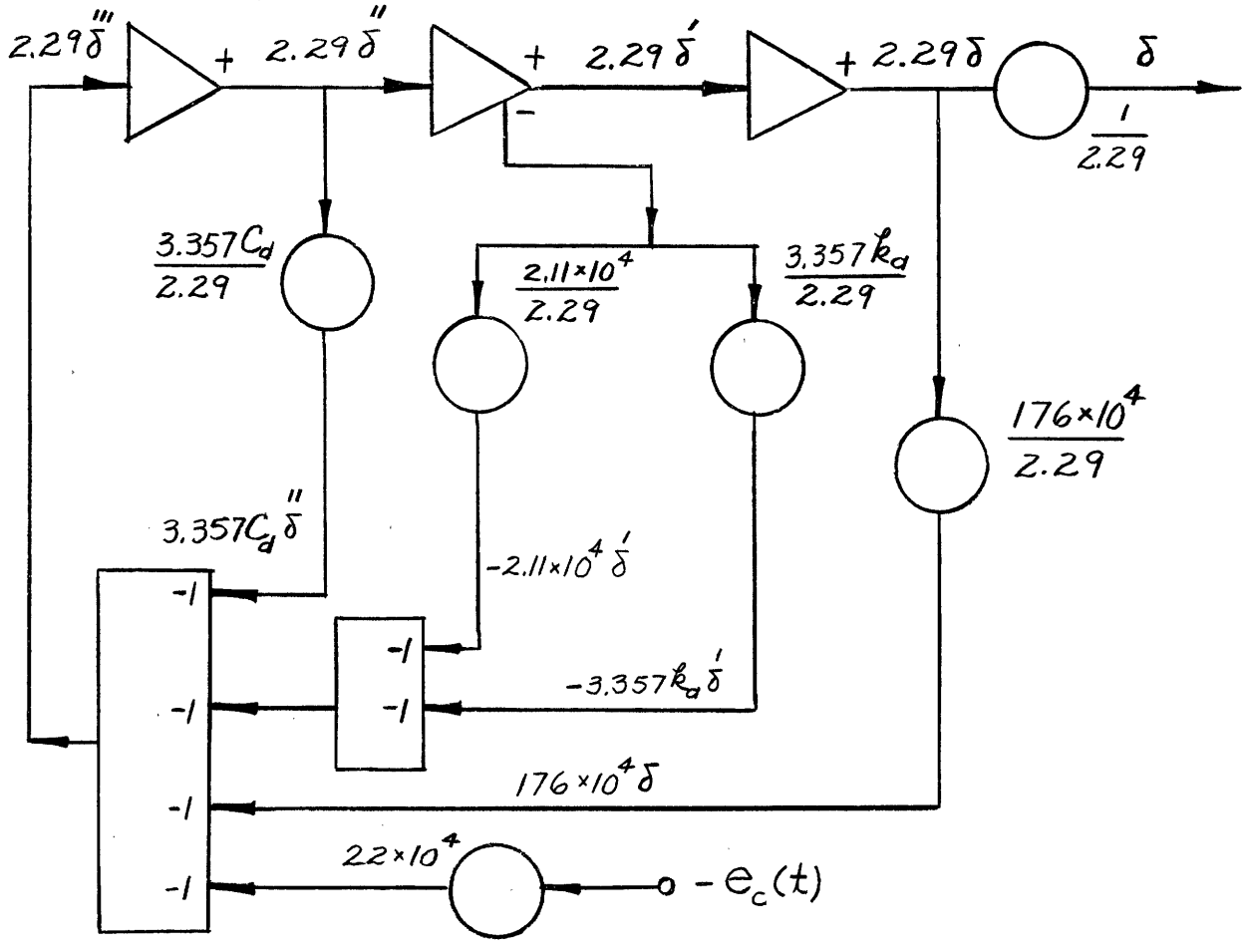

Fig. IV-2 Tentative simulator diagram for ideal hydraulic servo

The loop gain of the actual equation is too high; in order to simulate this equation, the time scale must be changed. Repalce p by 100 p, wo that the time dots on the computer's cathode ray oscillograph (ordinarily 2 seconds apart) now represent 2 sec/100 = 0.02 sec. (Time is "slowed down"). With this new time variable, equation (4-33) becomes

$$2.29p^3\delta = 0.22e_c - 0.03357C_d p^2\delta - (2.11+0.0003357k_a)p\delta - 176\times10^4\delta \qquad (4\text{-}34)$$

Further, let $$C_d = \frac{C_d}{C_{d_{ref}}} = \frac{C_d}{100} \qquad (4\text{-}35)$$

and $$k_a = \frac{k_a}{k_{a_{ref}}} = \frac{k_a}{10^5} \qquad (4\text{-}36)$$

Since the gain of potentiometers cannot exceed unity, amplifier gains may be employed to obtain the required numerical values for the constants. Fig. IV-2 then becomes Fig. IV-3(a).

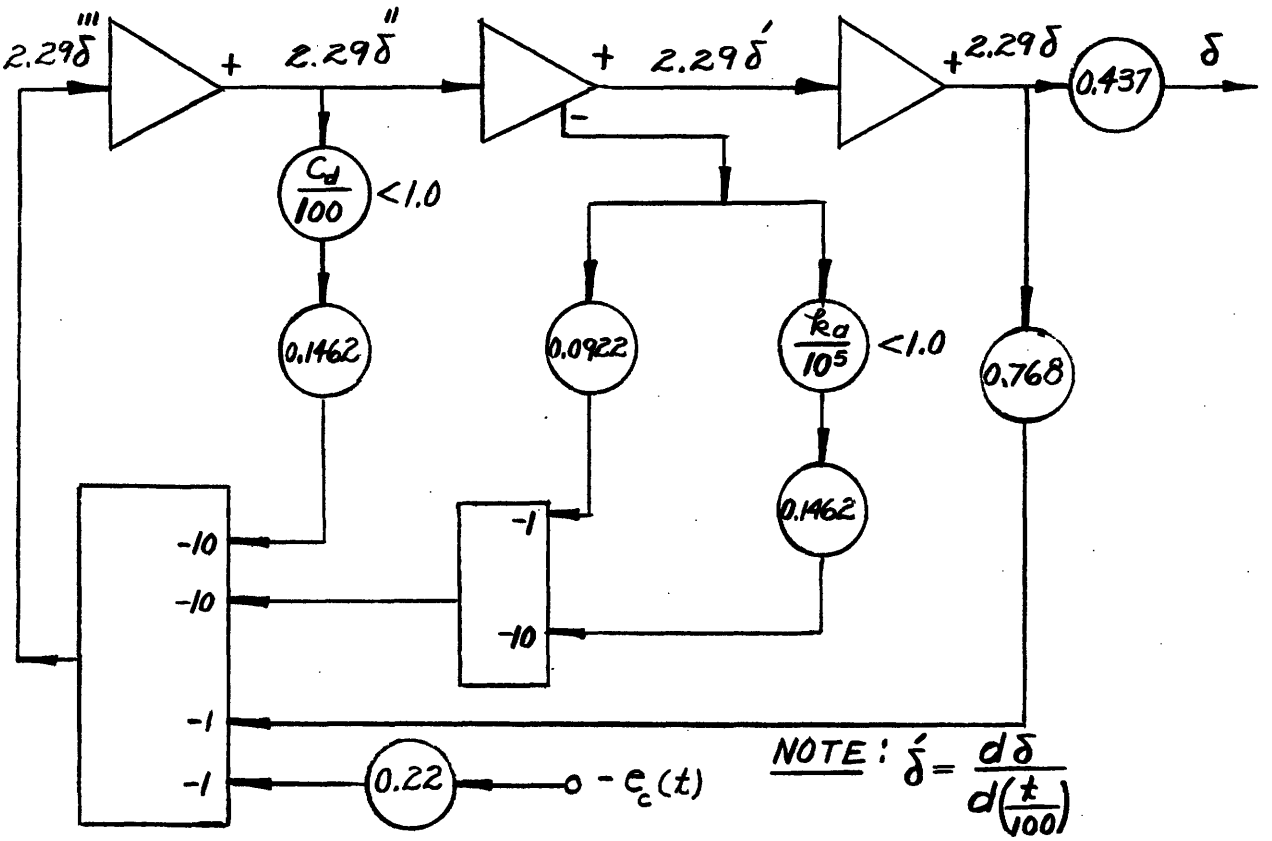

Fig. IV-3(a) Final simulator diagram for ideal hydraulic servo

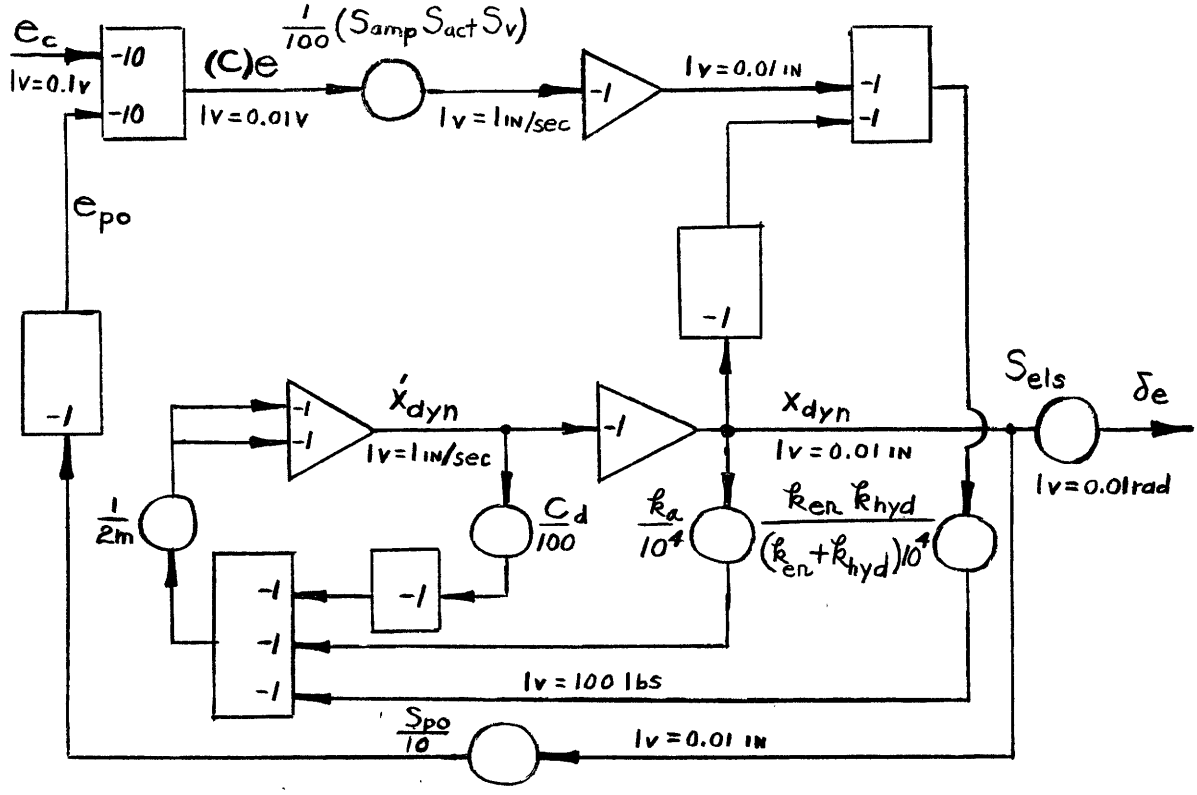

Since $\dot{V}_v = Q_v$, $[RF]_{[V_v;\, x_{dyn}]}$ may be obtained from $[RF]_{[Q_v;\, x_{dyn}]}$ (Eq. 2-16) as:

$$p[RF]_{[Q_v;x_{dyn}]} = [RF]_{[V_v;x_{dyn}]} = \frac{x_{dyn}}{V_v} = \frac{S_{act}k_{en}k_{hyd}}{m(k_{en}+k_{hyd})p^2+C_d(k_{en}+k_{hyd})p+k_{en}k_{hyd}+k_a(k_{en}+k_{hyd})}$$

Expanding:

$$\left[mp^2+C_dp+\left(\frac{k_{en}k_{hyd}}{k_{en}+k_{hyd}}+k_a\right)\right]x_{dyn} = V_v\left[S_{act}\frac{k_{en}k_{hyd}}{k_{en}+k_{hyd}}\right]$$

Also since $V_v = S_{amp}S_v[p](e_c - e_{po})$, it is seen that the above figure represents the ideal servo of Fig. II-14. Numerical constants in the figure are time and scale factors. See Section A of this Chapter for parameter values.

Fig. IV-3(b) Final simulator diagram modified for ideal hydraulic servo

The above arrangement permits instantaneous observation of δ (and its various derivitives) as C_d, k_a, and e_c are varied.

The preceding derivations serve to illustrate simulation techniques; however, the simulator schematic as given in Fig. IV-3(a) should be modified for two reasons:

(1) Ease of parameter variation

(2) Facilitation of addition of nonlinearities

A modified schematic is shown in Fig. IV-3(b) which includes notes explaining the change.

C. Simulation of the Nonlinear Hydraulic Servomechanism

Once again, a piece-by-piece study is helpful, and the block diagram for the system is repeated (Fig. IV-4).

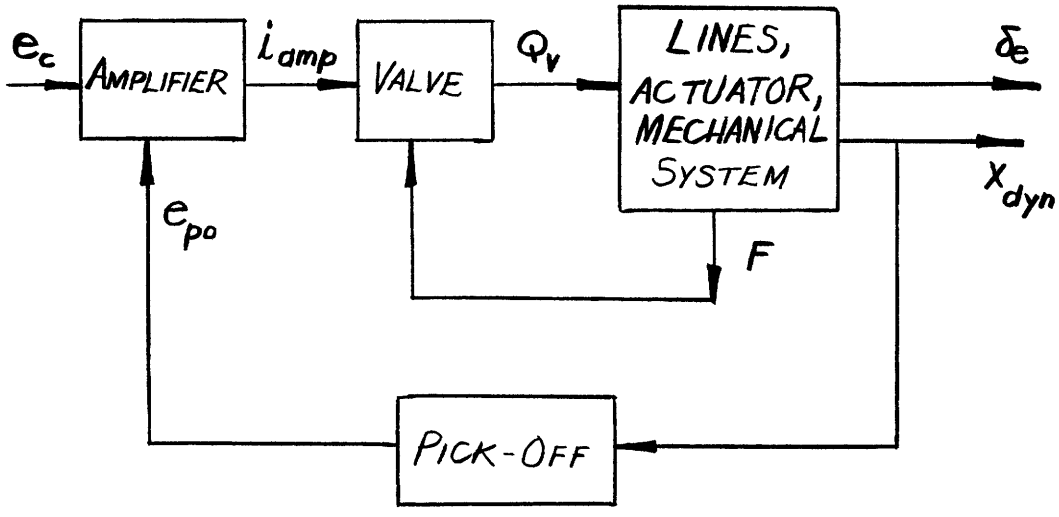

Fig. IV-4 Block diagram of nonlinear hydraulic servo

a. Amplifier. The amplifier is represented on the analog by an inverter, coupled with a potentiometer for adjusting the gain. The amplifier also has its setting divided by i_{max}, so that the output is (i/i_{max}), for reasons described later. (The factor 75 involves scaling, not discussed here.) See Fig. IV-5.

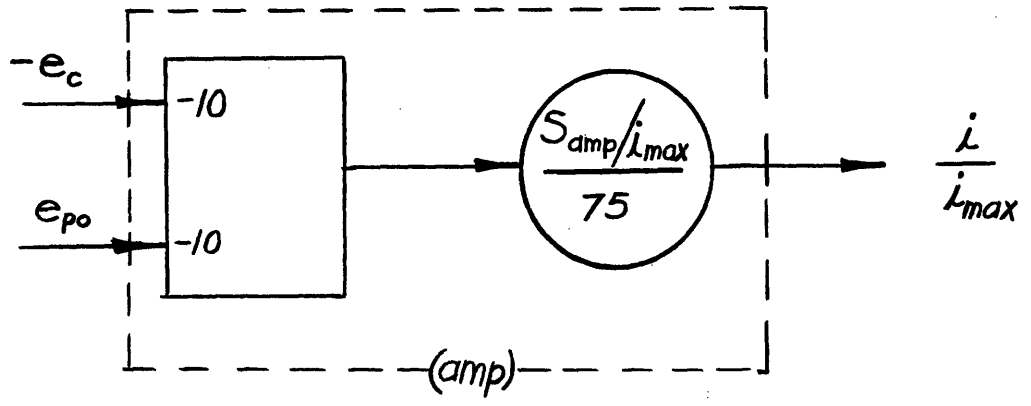

Fig. IV-5 Analog of Amplifier

b. Valve. The valve on the analog computer is composed of four sections: (1) two function generators which simulate the essential transfer characteristics of the valve orifices, (2) one multiplier which brings in the effect of pressure drop across the orifices with increasing load, (3) an integrator to sum up the flow rate, giving a volume of flow out, and (4) a second order unit to account for valve dynamics.

The inputs to the function generators are non-dimensionalized, so that at zero lap the function generators have a gain of unity for large inputs. This unit slope facilitates readjusting the lap and leakage after the sensitivity of the valve has been set to a new value. The change in sensitivity is then accomplished by adjusting the setting of the potentiometer in the amplifier analog circuit.

Lap and leakage must also be set on these function generators, in addition to the slope at low input currents. By utilizing an electronic multiplier, Q_v is obtained, which is the flow under load conditions from the valve (Fig. IV-6).

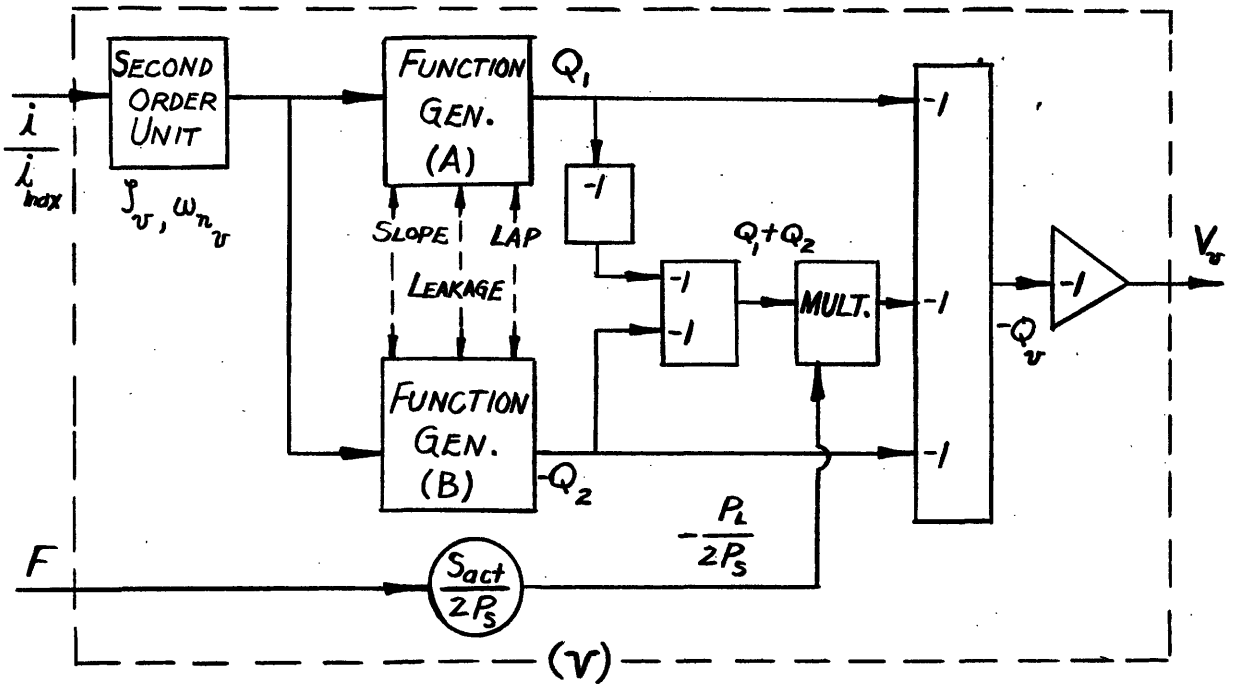

Fig. IV-6 Analog of valve

Lap is adjusted by feeding D.C. voltage (adjustable) into the function generator along with i/i_{max}. The leakage may be increased or decreased by adding or subtracting a D.C. voltage from the output of the function generators. In the actual set-up used, the potentiometers were ganged so that lap and leadage could be set for both function generators A and B simultaneously.

Q_V is supplied to an integrator, which yields V_V, the valve volume output. Also, a second-order unit is inserted into the input circuit to approximate the valve dynamics (due mostly to the hydraulic amplifier incorporated in the valve).*

Dither is added by summing an alternating current with i/i_{max} and applying the resultant current to the function generator.

c. Lines, Actuator, and Mechanical System. The analog schematic is similar to that developed in the ideal case (section B), except that only two integrations are used, since the valve is assumed to have a volume output, rather than a flow rate (as was assumed in

* The parameters for this second-order unit were obtained from direct frequency measurements of a typical valve (see Fig.IV-12A).

Fig. IV-3(a)). Also, coulomb friction is added here. (Fig. IV-7)

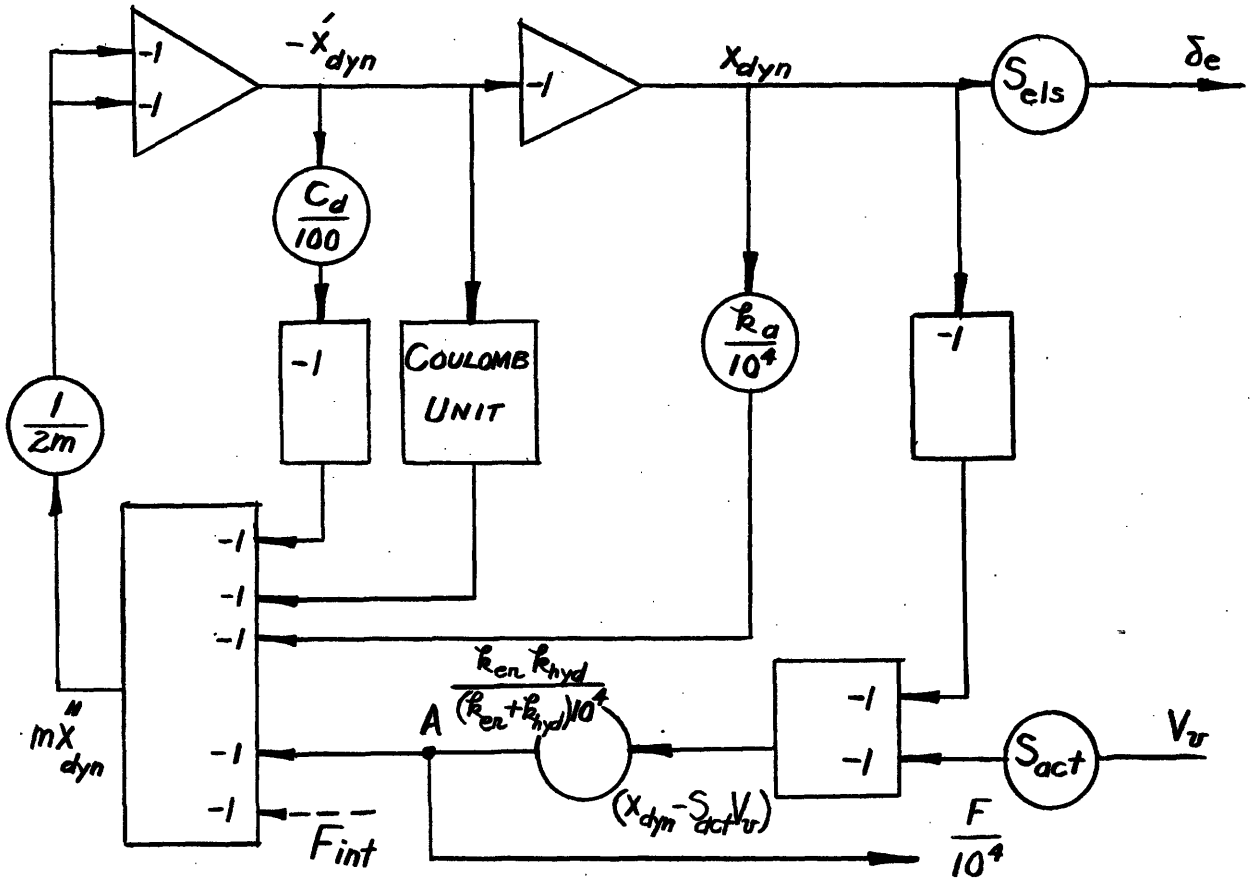

Fig. IV-7 Analog of lines, actuator, and mechanical system

The inverter at the lower left hand corner of this diagram actually serves as a force summing member. The force this member exerts on the actuator actually causes both the compression of the fluid and pressure drop across the orifices.

The equation represented above is as follows:

$$p^2 x_{dyn} + \frac{C_d}{m \cdot 10^2} p\, x_{dyn} + \frac{k_a}{m \cdot 10^4} x_{dyn} = \frac{k_{hyd} k_{er}}{(k_{hyd}+k_{er}) m \cdot 10^4} (S_{act} V_v - x_{dyn}) \tag{4-37}$$

$$\text{but} \quad F_{dyn} = m \cdot 10^4 p^2 x_{dyn} + \frac{C_d}{10^2} p\, x_{dyn} + \frac{k_a}{10^4} x_{dyn} \tag{4-38}$$

$$\therefore \frac{F_{dyn}}{10^4} = \frac{k_{hyd}k_{er}}{(k_{hyd}+k_{er})\ 10^4}(S_{act}V_v - x_{dyn}) \qquad (4\text{-}39)$$

consequently F_{dyn} may be obtained conveniently from point "A" on the diagram. Further refinements, as discussed in Section D, were later made in order to better approximate viscous friction effects, and to relocate the pick-off.

Coulomb friction is simulated by first obtaining px_{dyn} on the analog. This quantity is readily available as the output of the first integrator in Fig. IV-7. Now we want the coulomb friction to have a sign which will oppose motion, or expressed another way, we want it to have the same sign as the viscous damping term at the same instant.

$$F_{coulomb} = C\frac{\dot{x}_{dyn}}{|\dot{x}_{dyn}|} \qquad (4\text{-}40)$$

where C is a constant for a given system, in pounds of force.

The quantity $p\,x_{dyn}$ ($\dot{x}_{dyn}$) is amplified greatly, then clipped at the value set for C. The resultant voltage represents approximately the force exerted by coulomb friction upon the force summing member, for example, the actuator piston (Fig. IV-8)

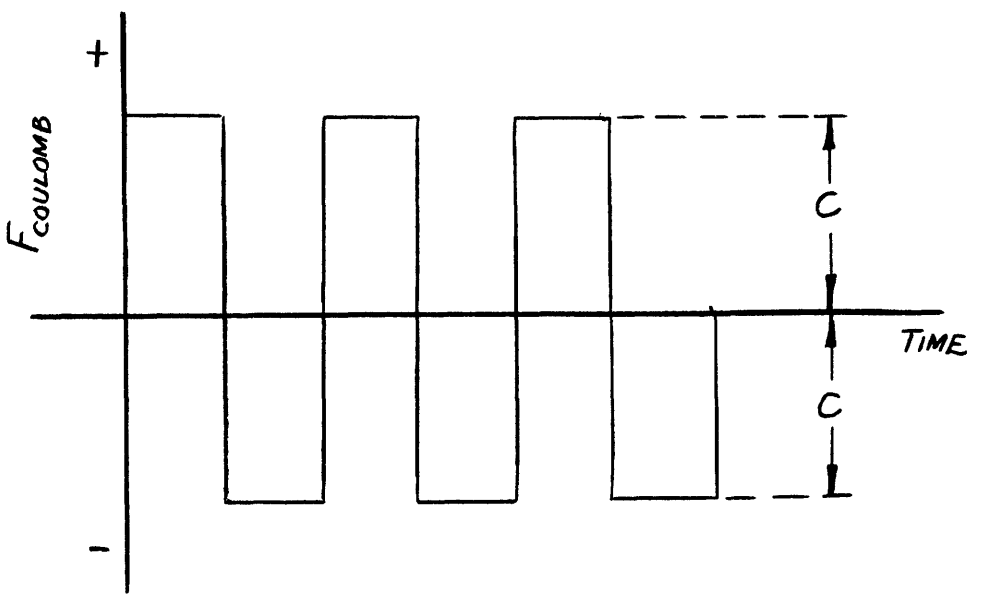

Fig. IV-8 Coulomb friction exerted upon a body with sinusoidal motion

d. Pick-Off. This is represented by a potentiometer; no diagram is necessary. Dynamics in this device are neglected.

D. Modifications of Original Simulator Circuit.

In the process of setting up the computer, it was felt that certain modifications should be made to investigate the effects of friction at the actuator (as contrasted with the effect of friction at the elevator linkage). Also, it seemed worthwhile to try locating the feedback pick-off at the actuator (rather than at the elevator linkage), thus placing part of the system dynamics outside of the loop. The effect of this change on stability and system response time could then be evaluated.

a. Addition of Friction at Actuator. A simple sketch of the mechanical system from valve to elevator is shown in Fig. IV-9.

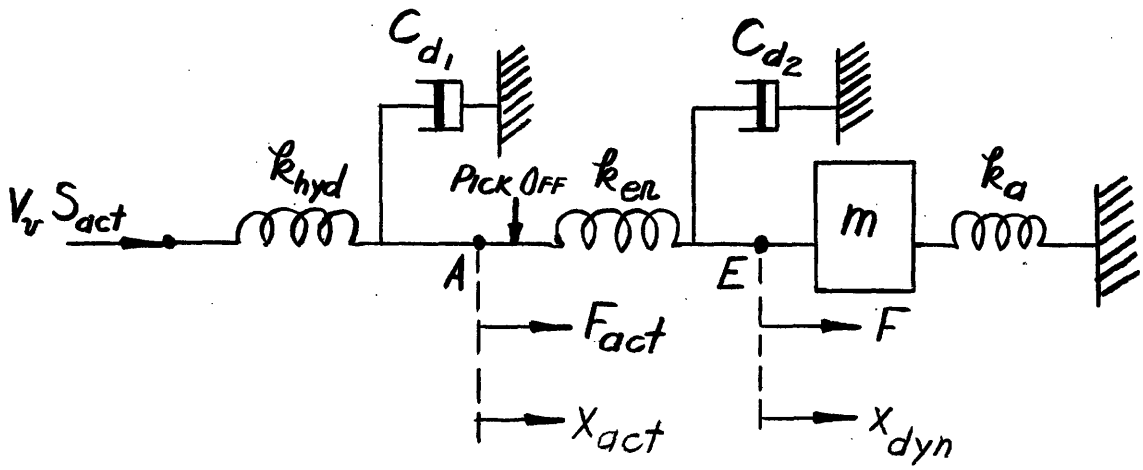

Fig. IV-9 Mechanical system showing friction at actuator and elevator

In the above figure, point A represents the location of the actuator, and point E represents the location of the elevator. The input displacement is seen to be $V_v S_{act}$ (The actuator sensitivity appears at this point since the volume output of the valve must be converted to an equivalent displacement). With displacement in-displacement out, the stiffness constants (k_{hyd}, k_{er}, k_a) may all be expressed in pounds per inch, making the relative effects of these three constants more easily studied.

With $V_v S_{act}$ as an input displacement, it is seen that the force

exerted upon A by the hydraulic fluid is

$$F_{hyd} = k_{hyd} (V_v S_{act} - x_{act}) \tag{4-41}$$

Tending to oppose motion is C_{d_1}, the viscous friction damping coefficient at the actuator (point A)

$$F_{C_{d_1}} = - C_{d_1} \dot{x}_{act} \tag{4-42}$$

The sum of these two forces, equations (4-41) and (4-42), is

$$F_{hyd} + F_{C_{d_1}} = k_{hyd} V_v S_{act} - x_{act} (p C_{d_1} + k_{hyd}) , \tag{4-43}$$

which must be balanced by the load forces transmitted through k_{er}.

The load forces exerted at E are simply

$$F_m + F_{C_{d_2}} + F_{k_a} = - x_{dyn} (mp^2 + C_{d_2} p + k_a) \tag{4-44}$$

where C_{d_2} is the viscous friction damping coefficient at the elevator, point E.

For equilibrium conditions, we must have

$$F_{hyd} + F_{C_{d_1}} = - (F_m + F_{C_{d_2}} + F_{k_a}) \tag{4-45}$$

or, substituting the expressions for the various forces in equation (4-45),

$$k_{hyd} V_v S_{act} - x_{act} (p C_{d_1} + k_{hyd}) = x_{dyn} (mp^2 + C_{d_2} p + k_a) \tag{4-46}$$

We see also from Fig. IV-9 that

$$x_{dyn} = x_{act} - (\text{compression of } k_{er})$$

or,

$$x_{dyn} = x_{act} - \frac{x_{dyn} (mp^2 + C_{d_2} p + k_a)}{k_{er}} \tag{4-47}$$

We now have two equations in two unknowns, x_{act} and x_{dyn}. Combining equations (4-46) and (4-47) we have

$$k_{hyd}V_vS_{act}-x_{dyn}\left(1+\frac{mp^2+C_{d_2}p+k_a}{k_{er}}\right)(pC_{d_1}+k_{hyd}) = x_{dyn}(mp^2+C_{d_2}p+k_a)$$

or, solving for x_{dyn}/V_v,

$$\frac{x_{dyn}}{V_v} = \frac{k_{hyd}S_{act}}{\left[(k_{hyd}+C_{d_1}p)\left(1+\frac{mp^2+C_{d_2}p+k_a}{k_{er}}\right)+(mp^2+C_{d_2}p+k_a\right]} \qquad (4\text{-}48)$$

which may be expressed in better form as

$$\frac{x_{dyn}}{V_v} = \frac{k_{er}k_{hyd}S_{act}/(k_{hyd}+k_{er}+C_{d_1}p)}{mp^2+C_{d_2}p+k_a+\frac{(k_{hyd}+C_{d_1}p)k_{er}}{(k_{hyd}+k_{er}+C_{d_1}p)}} \qquad (4\text{-}49)$$

To facilitate the addition of C_{d_1} to the existing analog wiring diagram with a minimum of rewiring, we rewrite the numerator and the last term of the denominator of eqn. (4-49)

$$\frac{k_{er}k_{hyd}S_{act}}{k_{hyd}+k_{er}+C_{d_1}p} = \left[\frac{k_{hyd}k_{er}}{k_{hyd}+k_{er}}\right]\left[\frac{1}{1+\left(\frac{C_{d_1}p}{k_{hyd}+k_{er}}\right)}\right]S_{act} \qquad (4\text{-}50)$$

and

$$\frac{(k_{hyd}+C_{d_1}p)k_{er}}{k_{hyd}+k_{er}+C_{d_1}p} = \left[\frac{k_{hyd}k_{er}}{k_{hyd}+k_{er}}\right]\left[\frac{1}{1+\left(\frac{C_{d_1}p}{k_{hyd}+k_{er}}\right)}\right]\left[1+\frac{C_{d_1}p}{k_{hyd}}\right] \qquad (4\text{-}51)$$

Equation (4-50) indicates that a first-order lag, $\left[\frac{1}{1+\left(\frac{C_{d_1} p}{k_{hyd}+k_{er}}\right)}\right]$, must be inserted in series with the potentiometer representing $\left(\frac{k_{er} k_{hyd}}{k_{er}+k_{hyd}}\right)$ in the analog circuit. Equation (4-51) shows that the only other circuit modification is the addition of a first order lead, $1+\frac{C_{d_1} p}{k_{hyd}}$, in the direct connection between x_{dyn} and summing amplifier R in Fig. IV-10. As seen from this figure, the first order lead was formed by merely leaving the direct connection to amplifier R (thereby feeding x_{dyn} into R), obtaining px_{dyn} at another point in the circuit, multiplying it with a potentiometer by $\left(\frac{C_{d_1}}{k_{hyd}}\right)$, and finally connecting that signal to amplifier R (thereby feeding $\left(\frac{C_{d_1} p}{k_{hyd}}\right)$ into R). The resultant signal coming out of summing amplifier R, neglecting a sign change, is then $x_{dyn}\left(1+\frac{C_{d_1} p}{k_{hyd}}\right)$.

b. Relocation of Pick-Off at Actuator

From equation (4-47) we have

$$x_{act} = x_{dyn} + \frac{1}{ker}\left(mp^2 x_{dyn} + C_{d_2} p x_{dyn} + k_a x_{dyn}\right)$$

It is seen that the quantity A in Fig. IV-10 is

$$A = -\left(mp^2 x_{dyn} + C_{d_2} p x_{dyn} + k_a x_{dyn}\right),$$

therefore

$$x_{act} = x_{dyn} - \frac{A}{ker}$$

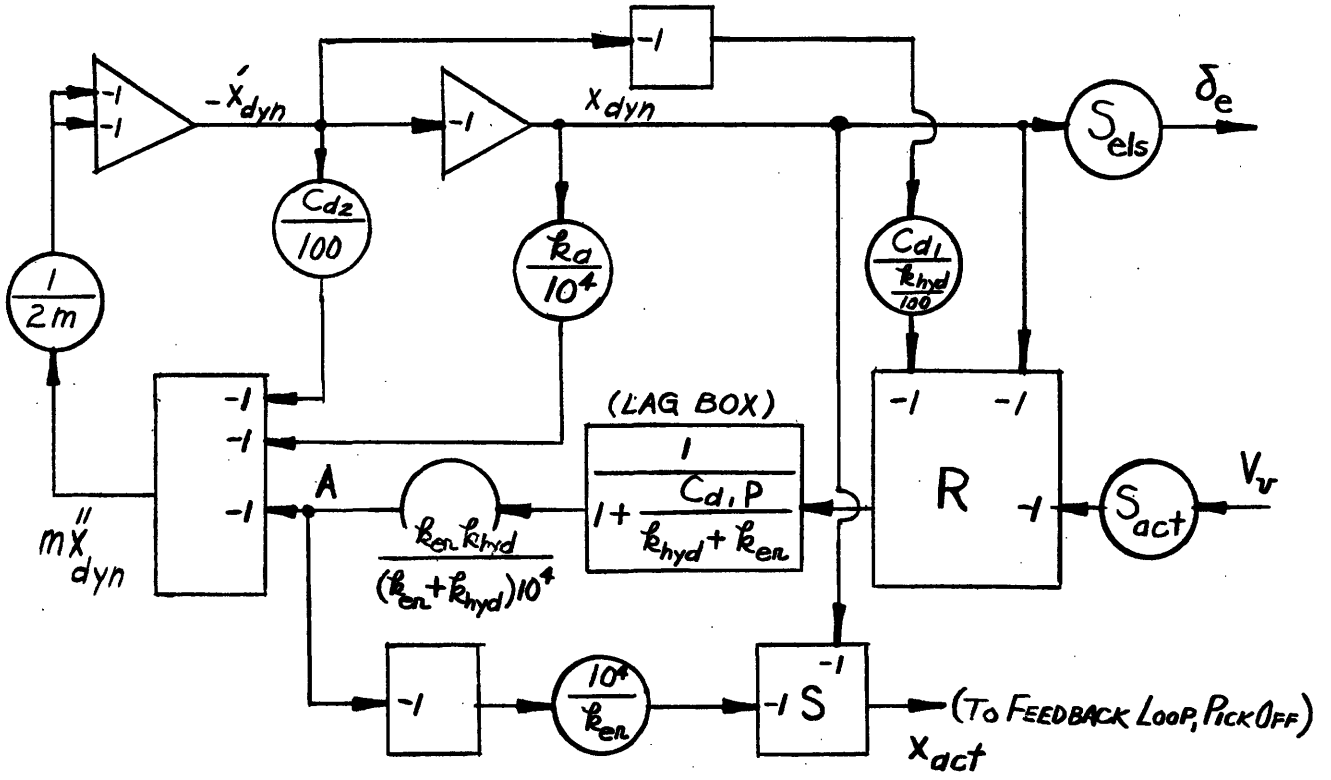

Fig. IV-10 Modified analog of lines, actuator, and mechanical system

x_{act} is thus easily obtained from summing amplifier S, as shown. (Numerical factors refer to scaling, which will not be discussed here.)

Fig. IV-11 is a schematic of the final simulator set-up. Potentiometer, integrator, and amplifier designations refer to the actual GPS computer used; Fig. IV-12 gives the frequency response and average leakage characteristic of a typical hydraulic valve.

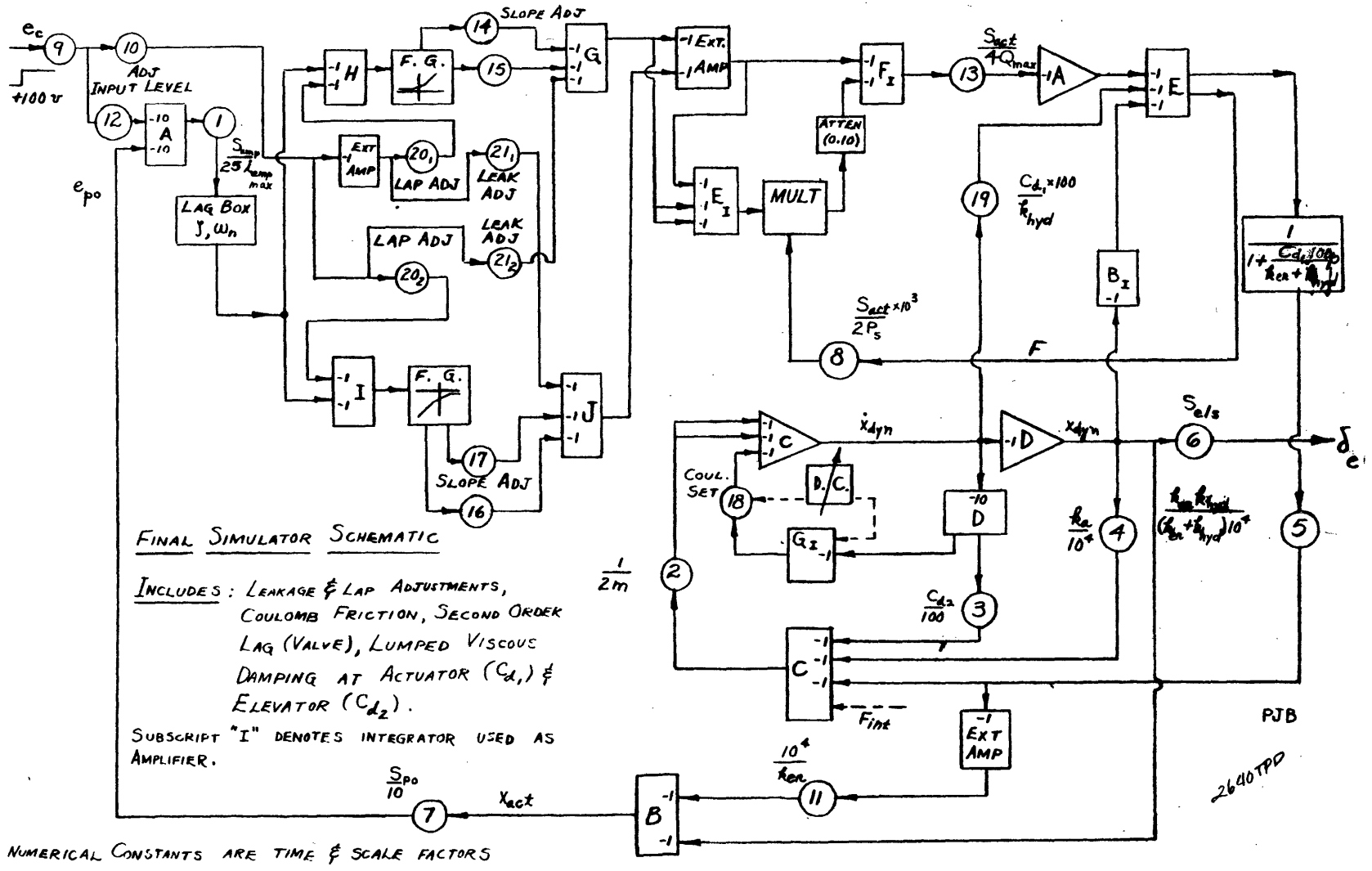

Fig. IV-11 Final simulator schematic

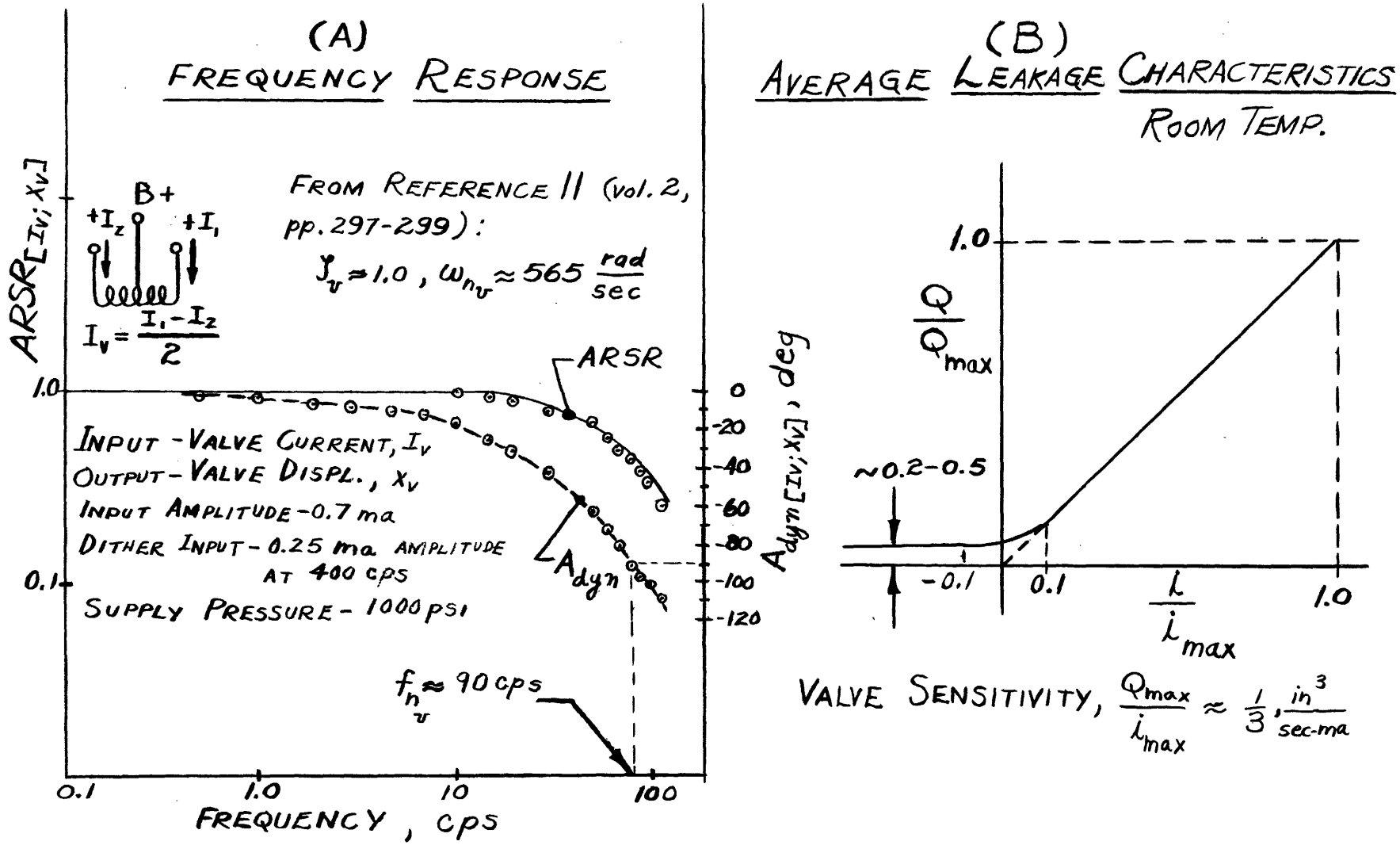

Fig. IV-12 Measured frequency response & average leakage characheristics of typical hyraulic valve

CHAPTER V

DATA

A. Ideal Hydraulic Servo

Figs. V-1, (A-J), are photographs of various responses obtained for an "ideal" servo (i.e., one whose valve characteristic is given by $Q_v = ki_{amp}$); the pick-off is placed at the elevator and the actuator contains no viscous damping. The system is as represented in Fig. IV-3(b), with all constants as calculated in Chapter IV except for the following parameters which were varied:

1) $\frac{S_v S_{amp} S_{act}}{S_{ref}}$, where $S_{ref} = 100$

2) $\frac{C_d}{C_{d_{ref}}}$, where $C_{d_{ref}} = 1000$

3) $\frac{k_a}{k_{a_{ref}}}$, where $k_{a_{ref}} = 10,000$

With this system, optimum response time (measured as 0.056 secs) was obtained with $\frac{S_v S_{amp} S_{act}}{S_{ref}} = 0.1$, $\frac{C_d}{C_{d_{ref}}} = 0.088$ and $\frac{k_a}{k_{a_{ref}}} = 0.05$. Values of these parameters selected for response

study are:

$$\frac{S_v S_{amp} S_{act}}{S_{ref}} = 0.4 , \ 0.088 , \text{ and } 0.2$$

$$\frac{C_d}{C_{d_{ref}}} = 0.03 , \ 0.1 , \text{ and } 0.4$$

$$\frac{k_a}{k_{a_{ref}}} = 0.05 , \ 0.30 , \text{ and } 0.60 ,$$

with $\frac{k_a}{k_{a_{ref}}}$ the variable on each photograph. The following conditions hold for each photograph (highest values of $\frac{k_a}{k_{a_{ref}}}$ correspond to response curves of greatest damping):

	$\frac{S_v S_{amp} S_{act}}{S_{ref}}$	$\frac{C_d}{C_{d_{ref}}}$	$\frac{k_a}{k_{a_{ref}}}$
Photo A)	.04	.03	.05
			.30
			.60
B)	.04	.10	.05
			.30
			.60
C)	.04	.40	.05
			.30
			.60
D)	.088	.03	.05
			.30
			.60
E)	.088	.10	.05
			.30
			.60
F)	.088	.40	.05
			.30
			.60

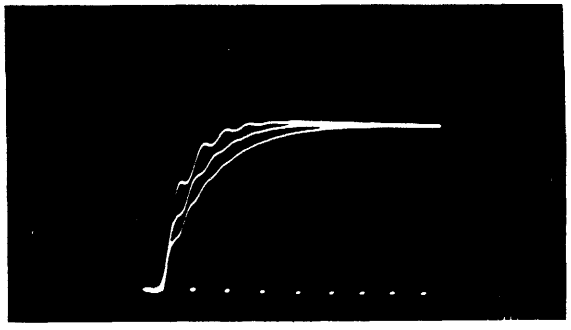

A

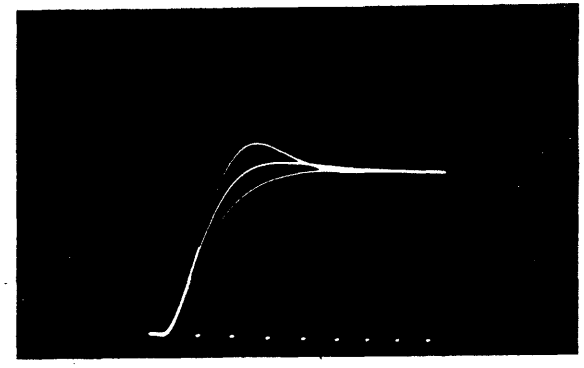

C

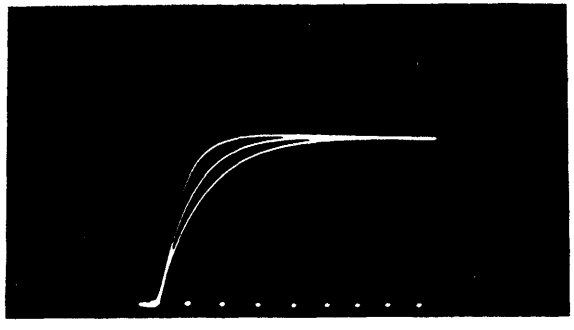

B

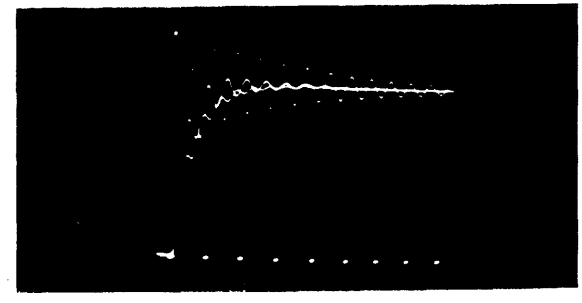

D

Fig. V-1 Ideal system responses.

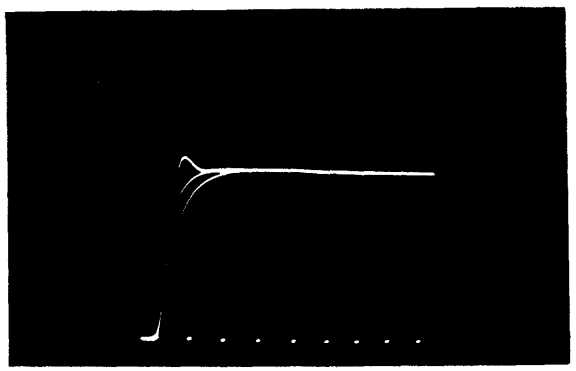

E

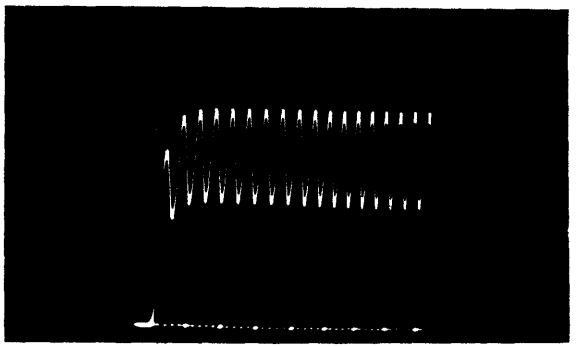

G

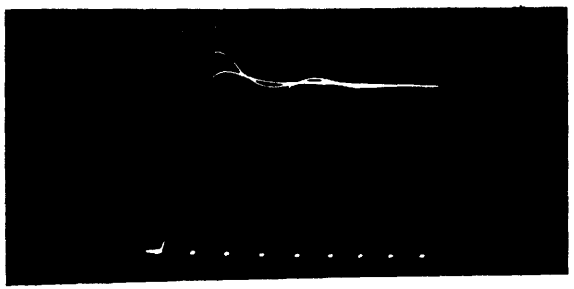

F

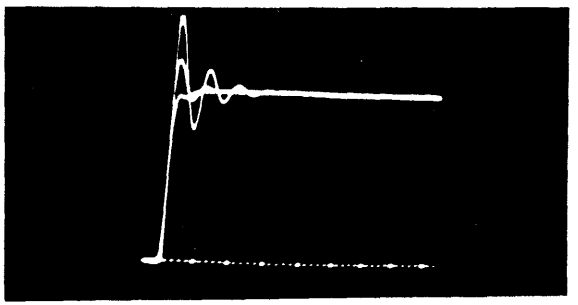

H

Fig. V-1 Ideal system responses. (cont.)

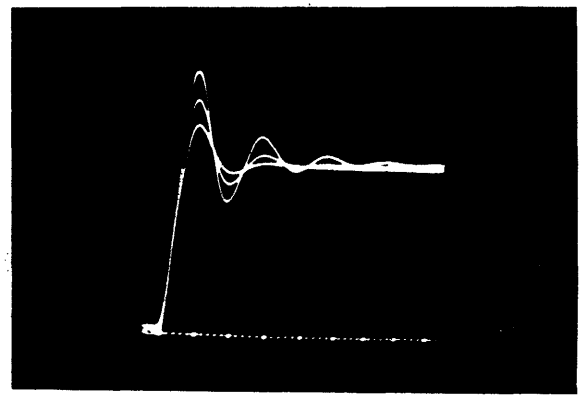

I

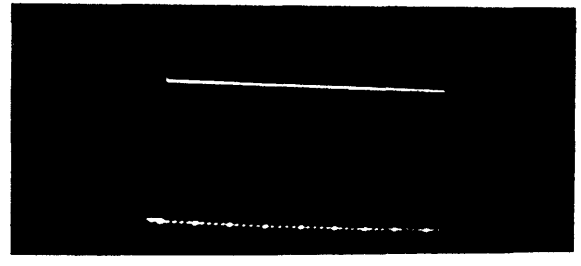

J

Fig. V-1 Ideal system responses. (cont.)

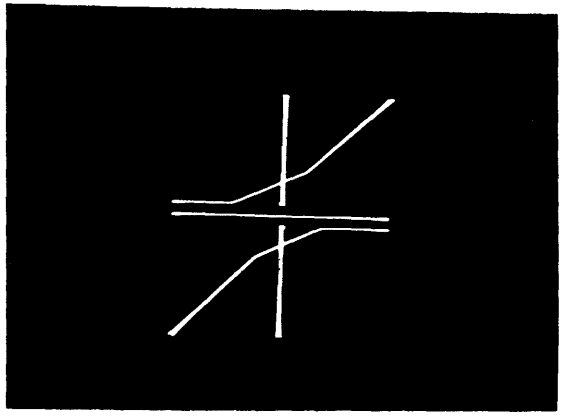

This figure is a composite photo showing the transfer characteristics of two function generators (see Fig. IV-11 for location of both generators in the simulator schematic). Arbitrary values of leakage and underlap are indicated for illustrative purposes; these characteristics represent both orifices of a valve. Compare with transfer characteristics of typical hydraulic valve (Fig. IV-12B).

Fig. V-2 Function generator's transfer characteristics.

	$\frac{S_v S_{amp} S_{act}}{S_{ref}}$	$\frac{C_d}{C_{d_{ref}}}$	$\frac{k_a}{k_{a_{ref}}}$
Photo G)	.20	.03	.05
			.30
			.60
H)	.20	.10	.05
			.30
			.60
I)	.20	.40	.05
			.30
			.60

J) Step Input of 2 volts for all the above responses.

B. Nonlinear Hydraulic Servo (Pick-Off at Actuator)

Fig. V-2 is a photograph of a typical "valve characteristic" as generated by the function generator used to obtain the nonlinear data that follows.

Figs. V-3,(A-DD)are photographs of the various responses obtained for a nonlinear servo; the pick-off is now placed at the actuator (and hench, elevator dynamics are not included in the closed loop), viscous damping is present at both the elevator and actuator, and coulomb damping has been included. Dither has been neglected since its effect was observed to be negligible. This may be explained on the basis of the fact that a balanced valve is considered in this problem. The system is as represented in Fig. IV-11. The following quantities were varied:

1) Pressure feedback (i.e., the effect of load upon the differential orifice pressure) under differenc aerodynamic loads; valve settings were zero lap and .02 leakage.
2) Aerodynamic load with different valve leakage and lap parameters.
3) Aerodynamic load with various coulomb and viscous damping values. (Valve set at .04 leakage and .2 underlap).

4) Magnitude of step input under different aerodynamic load and valve conditions.
5) Aerodynamic load with several valve underlap and leakage conditions.
6) Aerodynamic load with different elevator inertias and valve underlaps (Leakage set at .02).
7) Aerodynamic load with different valve underlaps (Viscous friction lumped at the actuator).
8) Aerodynamic load with different valve underlaps (With interfering moment at the elevator).

With reference to (1) above where the pressure feedback value of .49 is the calculated potentiometer setting; the command voltage was a step of 1.18 volts. The higher pressure feedback values correspond to the smoothest or most highly damped responses:

	$k_a/k_{a_{ref}}$	Pressure Feedback
Photo A)	0	0
		.49
B)	.05	0
		.49
C)	.30	0
		.49
D)	.60	0
		.49

With reference to (2) above with a command voltage step of 1.18 volts; increasing the load in each case smooths or dampens the response:

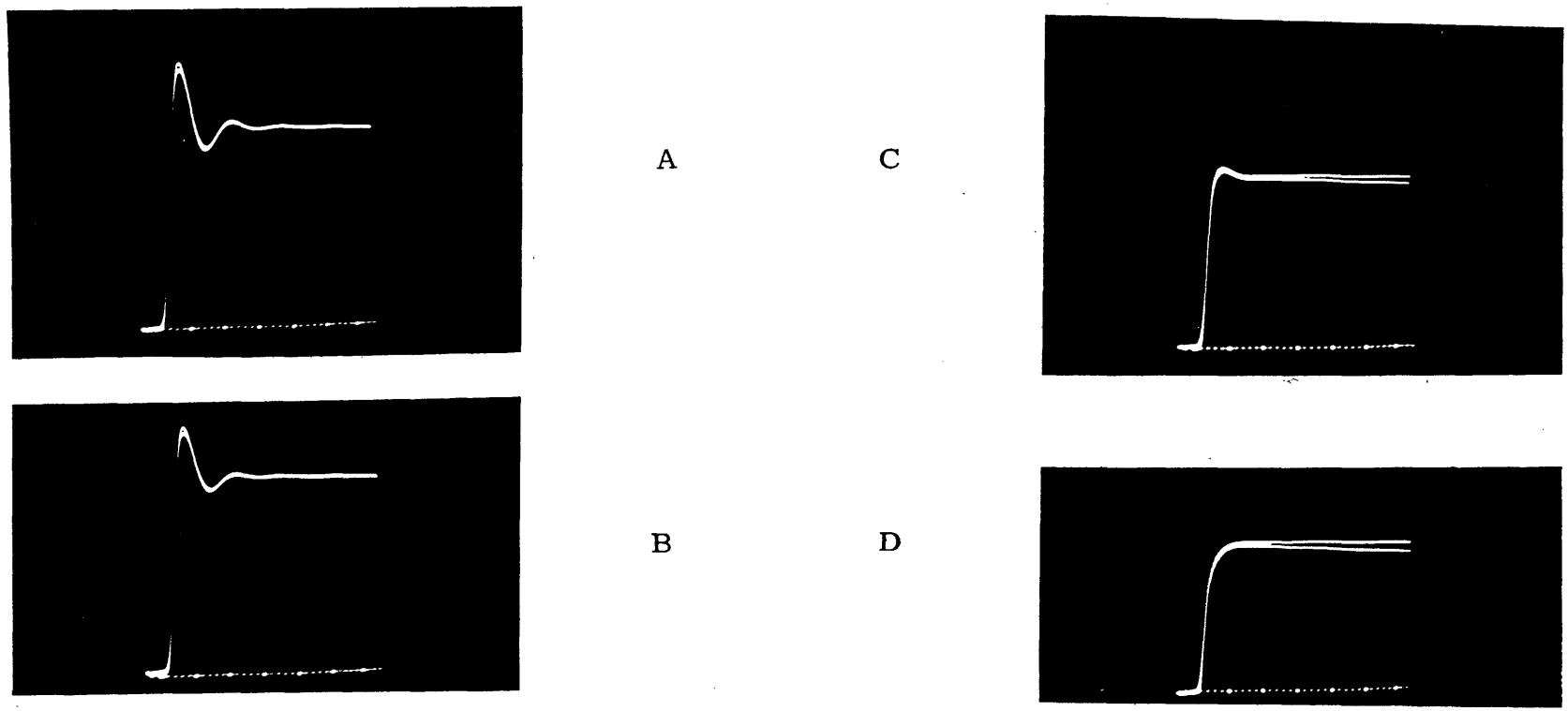

Fig. V-3 Nonlinear system responses.

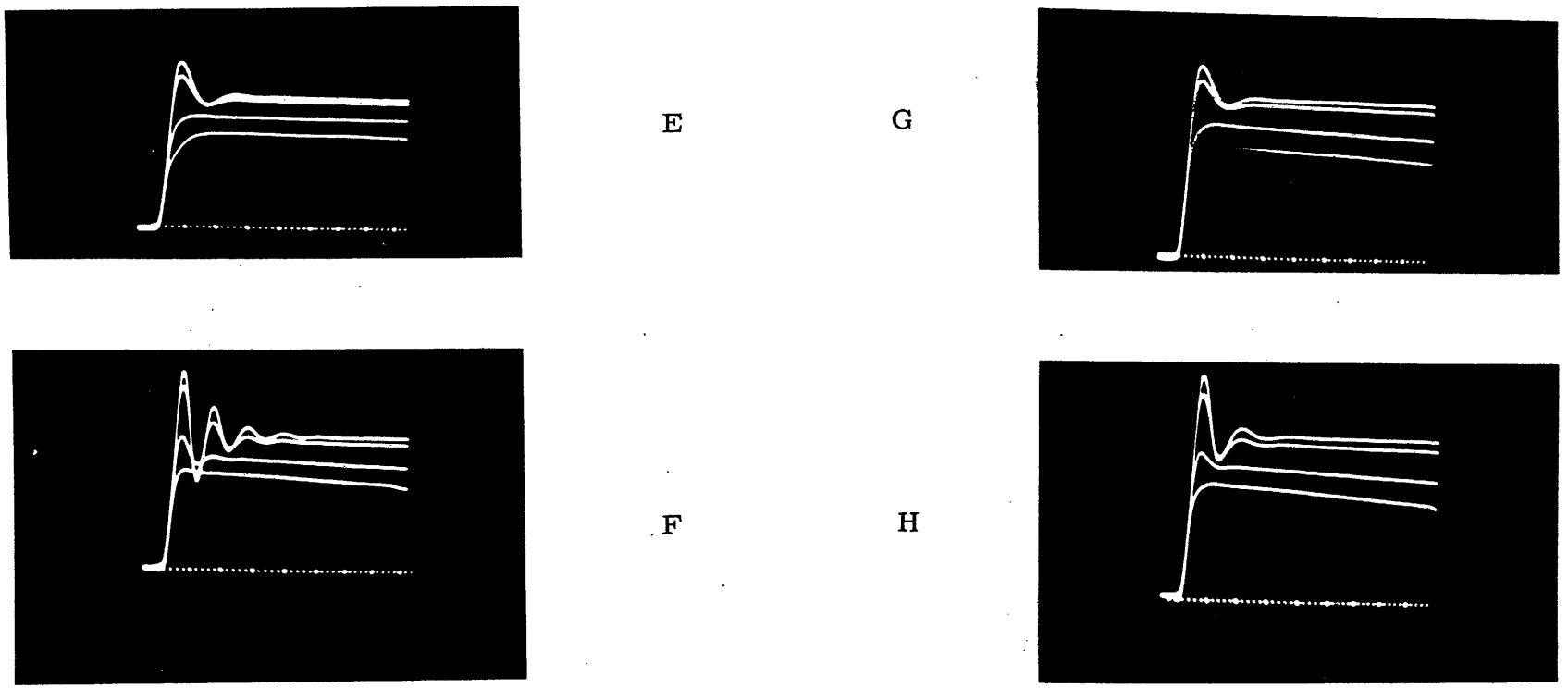

Fig. V-3 Nonlinear system responses. (cont.)

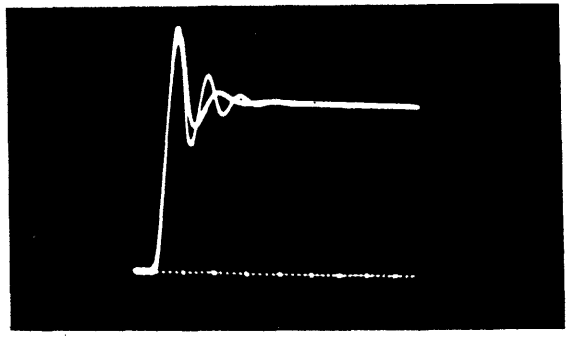

I

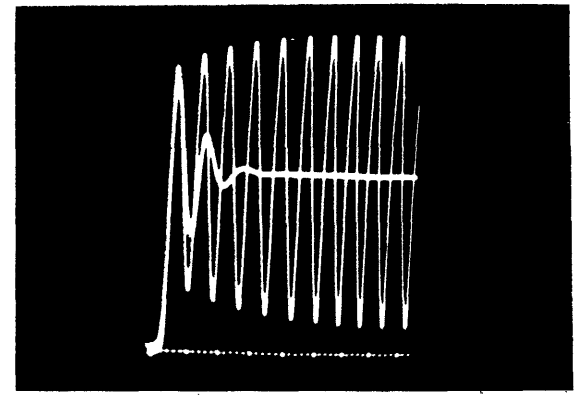

K

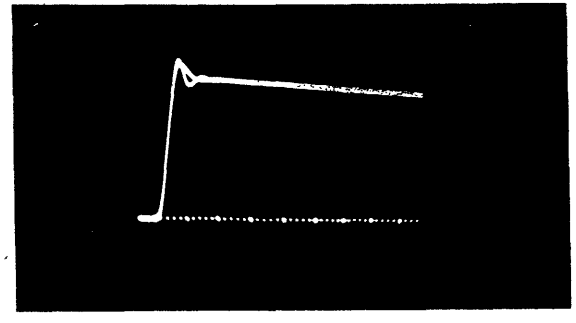

J

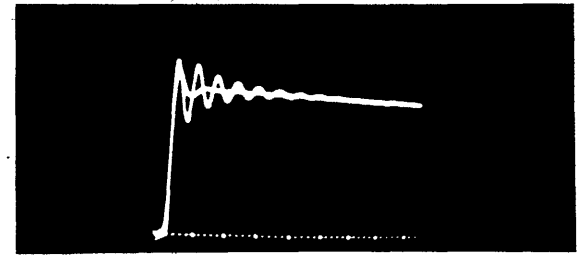

L

Fig. V-3 Nonlinear system responses. (cont.)

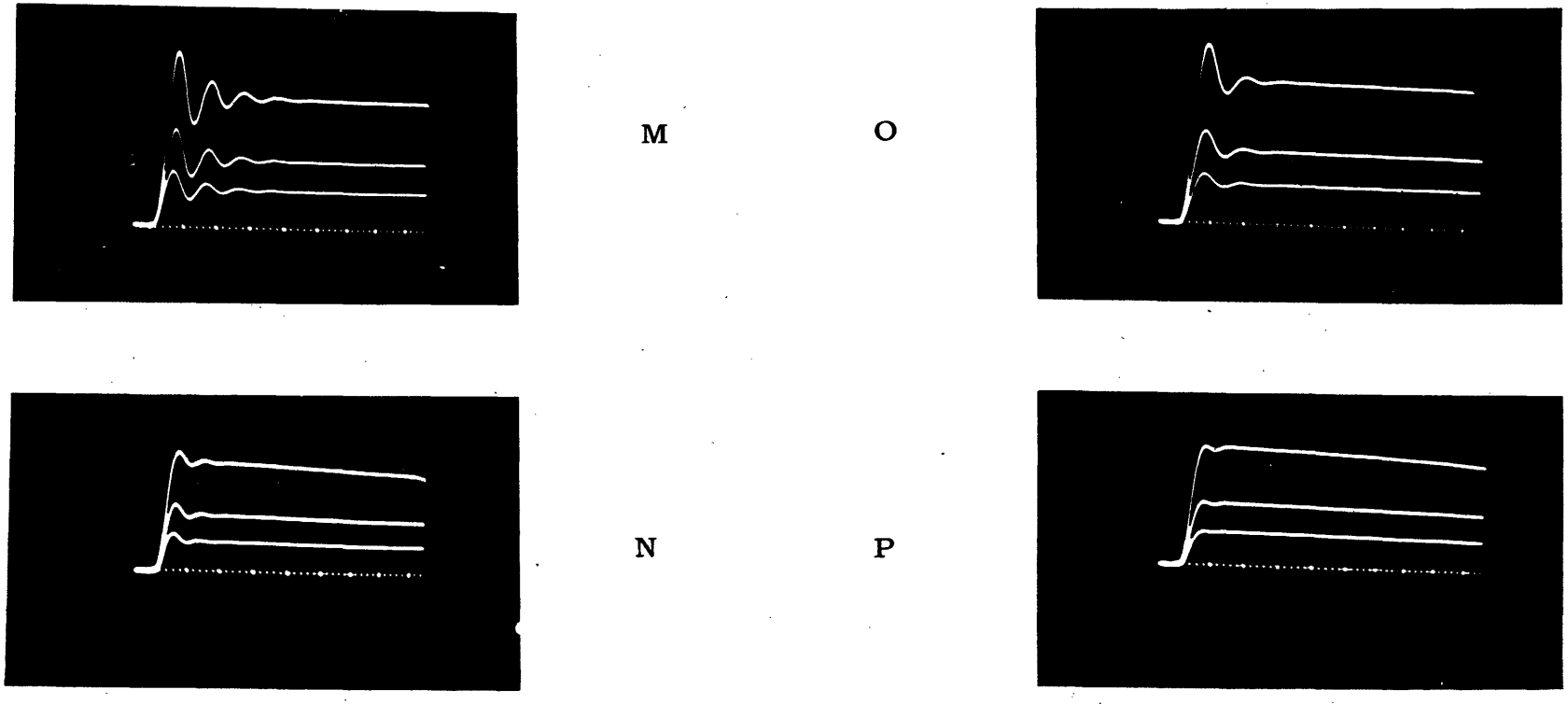

Fig. V-3 Nonlinear system responses. (cont.)

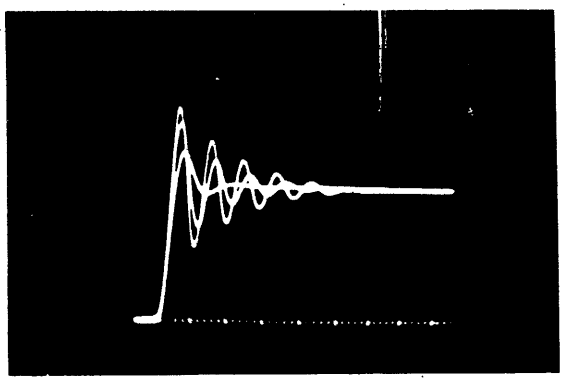

Q

S

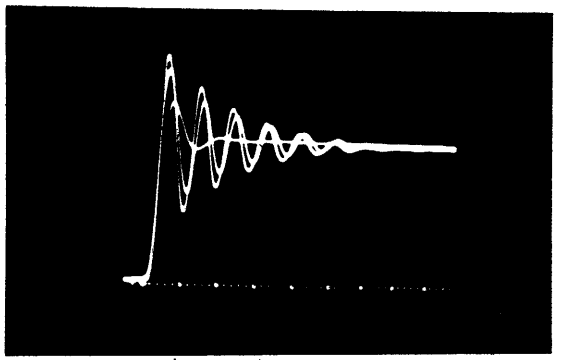

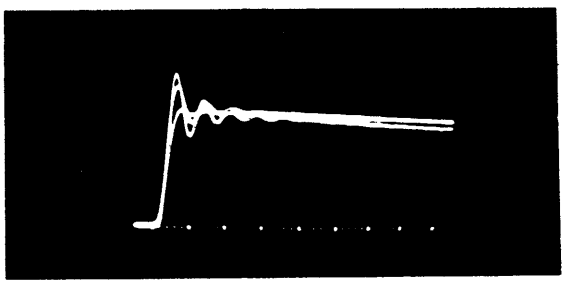

R

T

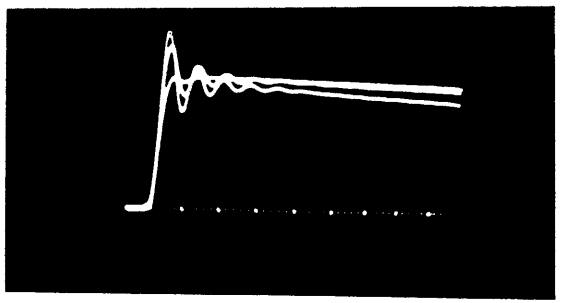

Fig. V-3 Nonlinear system responses. (cont.)

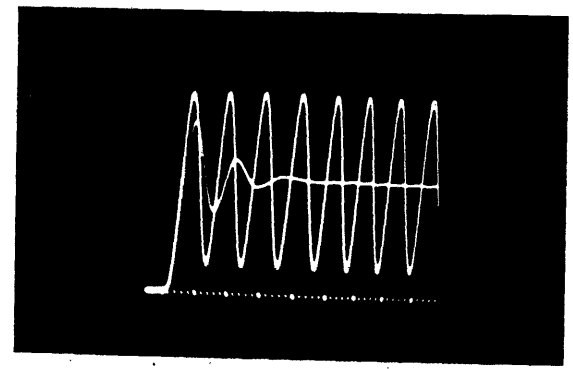

U

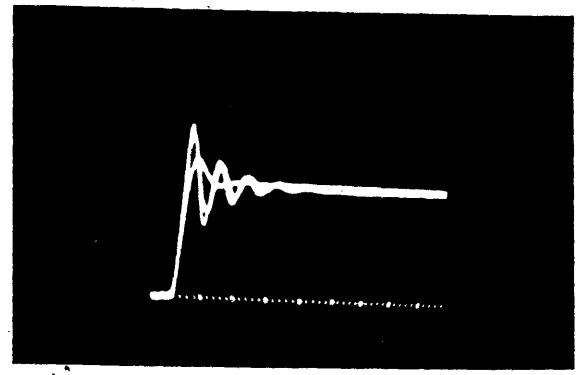

W

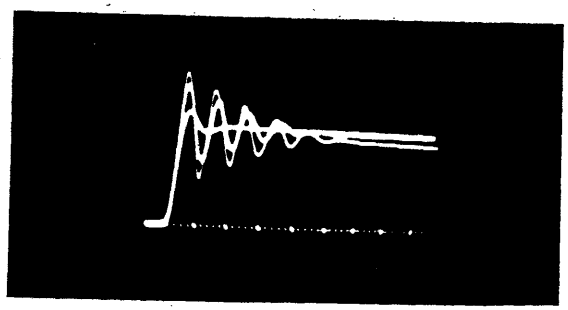

V

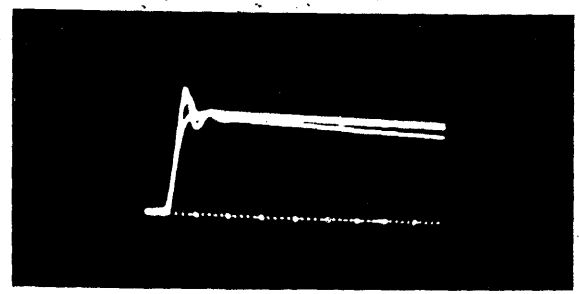

X

Fig. V-3 Nonlinear system responses. (cont.)

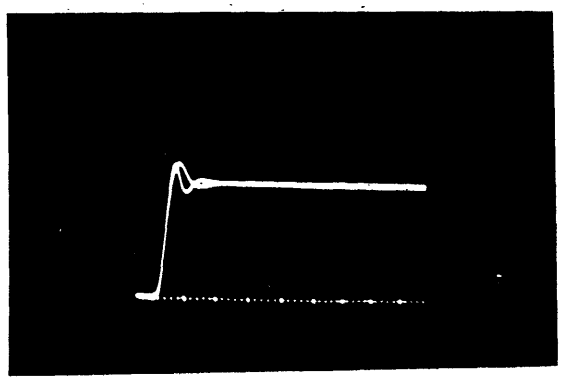

Y

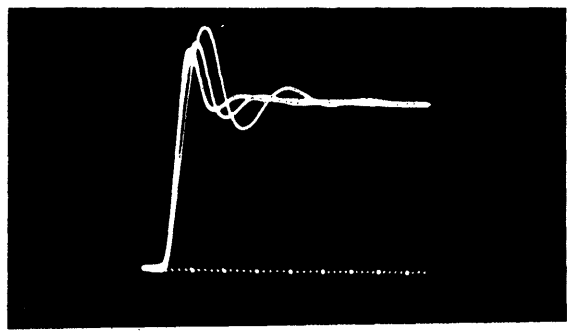

AA

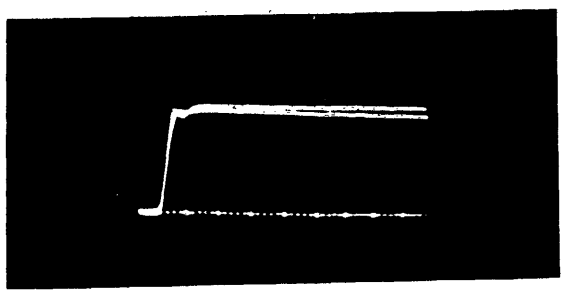

Z

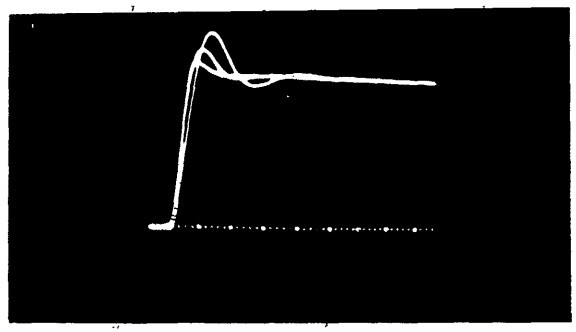

BB

Fig. V-3 Nonlinear system responses. (cont.)

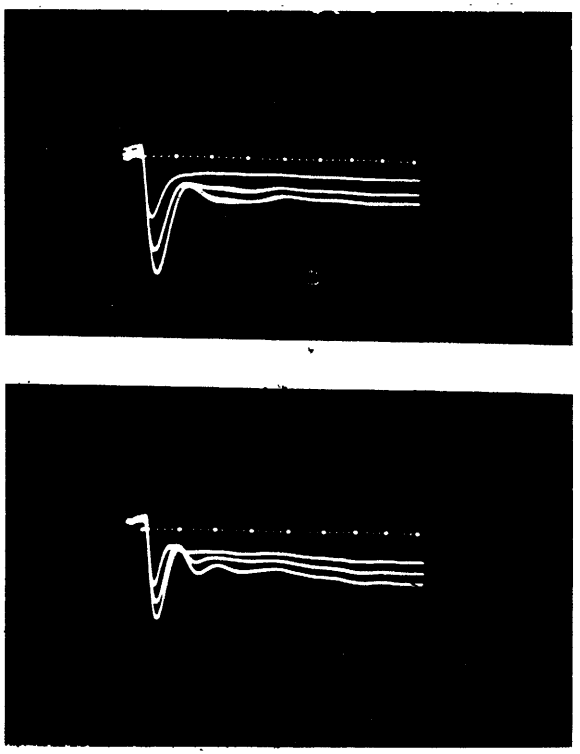

Fig. V-3 Nonlinear system responses (con't)

	$k_a/k_{a_{ref}}$	leakage	underlap
Photo E)	0	0	0
	.05		
	.30		
	.60		
F)	0	0	.2
	.05		
	.30		
	.60		
G)	0	.04	0
	.05		
	.30		
	.60		
H)	0	.04	.2
	.05		
	.30		
	.60		

With reference to (3) above with a measured frictional elevator hinge moment of 111 in.-lbs. corresponding to a voltage of .743 volts applied at the first integrator in the mechanical circuit; the command voltage was a step of 1.18 volts. The addition of coulomb damping in each case dampens the response:

	$k_a/k_{a_{ref}}$	$C_{d_1} = C_{d_2}$ $(\frac{\#sec}{in})$	Coloumb damping (volts)
Photo I)	0	50	.743
			0
J)	.3	50	.743
			0
K)	0	25	.743
			0
L)	.3	25	.743
			0

With reference to (4) above with viscous damping values of $50\ \frac{\#sec}{in}$; the highest value of step input corresponds to the highest final response in each case:

	Input step (v)	$k_{a/k_{a_{ref}}}$	leakage	underlap
Photo M)	.59 1.18 2.36	0	.04	2
N)	.59 1.18 2.36	.25	.04	2
O)	.59 1.18 2.36	0	.04	0
P)	.59 1.18 2.36	.25	.04	0

With reference to (5) above with a command voltage of 1.18 volts; the higher values of underlap correspond to the more oscillatory responses:

	$k_{a/k_{a_{ref}}}$	leakage	underlap
Photo Q)	0	.04	0 .3 .6
R)	.25	.04	0 .3 .6
S)	0	.02	0 .3 .6
T)	.25	.02	0 .3 .6

With reference to (6) above where the valve leakage is .02; the command voltage is a step of 1.18 volts. The higher values of underlap correspond to the more oscillatory responses:

	$k_a/k_{a_{ref}}$	elevator inertia ($\frac{\#sec^2}{in}$)	underlap
Photo U)	0	1.368	0
			.3
V)	.25	1.368	0
			.3
			.6
W)	0	.499	0
			.3
			.6
X)	.25	.499	0
			.3
			.6

With reference to (7) above where C_{d_2} = 50 #sec/in ; valve leakage is .02, valve underlap is zero and the command voltage is a step of 1.18 volts. The addition of C_{d_1} dampens the response:

	$k_a/k_{a_{ref}}$	C_{d_1} ($\frac{\#sec}{in}$)
Photo Y)	.05	0
		50
Z)	.25	0
		50
(AA)	.05	100
		200
		400
(BB)	.25	100
		200
		400

With reference to (8) above for a command voltage of zero and an interfering input of .5 volts corresponding to 50 lbs; the larger load

values correspond to the responses with the least negative final values:

	$k_a/k_{a_{ref}}$	underlap
Photo CC)	.05	0
	.20	
	.60	
DD)	.05	.3
	.20	
	.60	

C. Nonlinear Hydraulic Servo (Pick-Off at Elevator)

Figs. V-4, A-F are photographs of the various responses obtained for a nonlinear servo; the pick-off is placed at the elevator, hence, the elevator linkage system is now included in the loop. Tests were made under different lap conditions, with leakage set at .02. Both system response and pressure feedback to valve orifice were measured. In each case, the top photo represents the elevator response, and the bottom picture represents the quantity $\frac{1}{2}\frac{P_L}{P_s}$, where P_L is the pressure developed across the actuator driving the load.

	lap	$k_a/k_{a_{ref}}$
Photo A)&B)	0	0
		.05
		.3
		.6
C)&D)	.3	0
		.05
		.3
		.6
E)&F)	.6	0
		.05
		.3
		.6

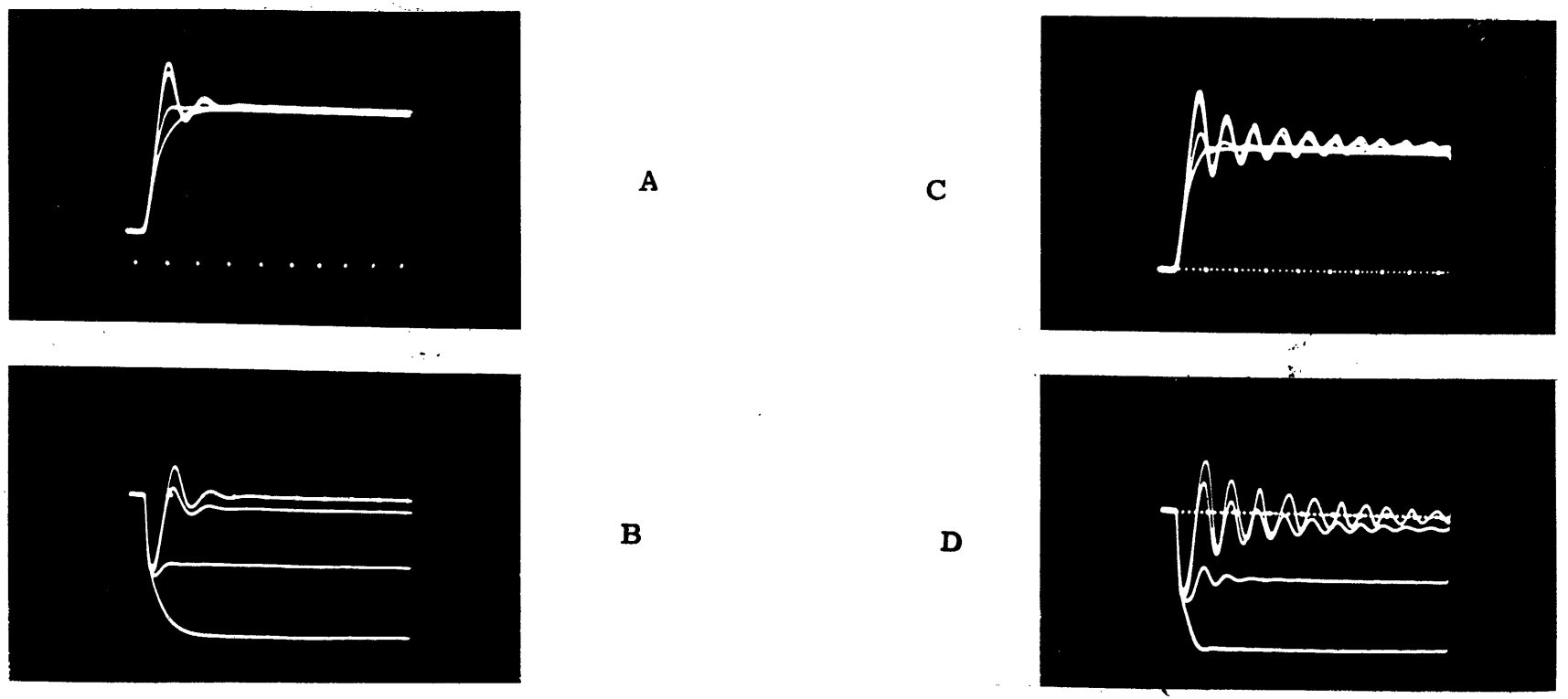

Fig. V-4 Nonlinear system responses (pick-off at elevator)

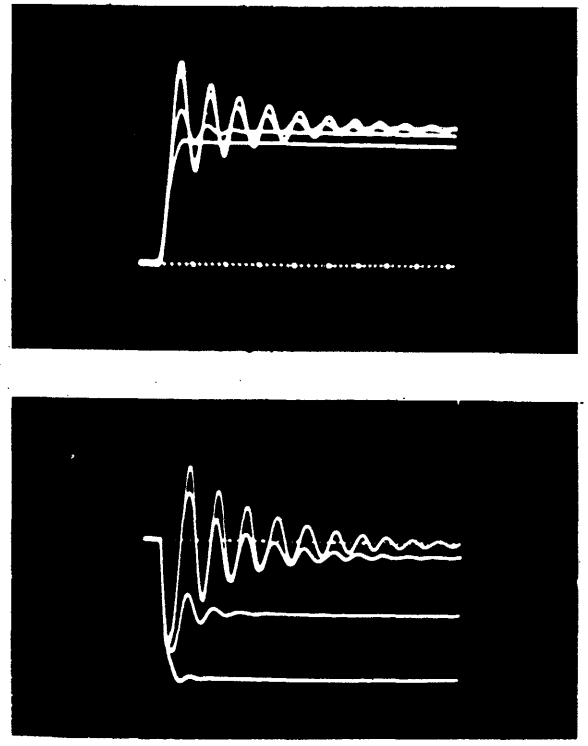

Fig. V-4 Nonlinear system responses (pick-off at elevator)(con't)

CHAPTER VI

CONCLUSIONS

A. Discussion of Results

1) Ideal System Responses

The ideal system responses are included principally for the purpose of comparison with the nonlinear responses to be presented later, and to serve as a check on the operation of the analog computer. However, certain general statements may be made about the system.

As shown in Chapter II, the ideal hydraulic servomechanism is a third order system; one integration is provided by the valve and two by the idealized second order mechanical system.

The change in response with increasing damping of the second order portion of the system gives evidence that for low values of C_d, increasing its value damps the response. For example, Fig. V-1(B) has a value three times that of Fig. V-1(A), and shows a considerably smoother response. However, Fig. V-1(C), which has thirteen times the damping value of Fig. V-1(A), actually shows a more oscillatory response than Fig. V-1(B). This can be explained by noting that C_d is the coefficient on the p^2 term in the performance equation, and is not effective as a damping coefficient. At low values it serves to smooth the response, but at higher values it tends to decrease the effect of the p^3 term, and as a result effectively reduces the third order system to a second order system. At this point, then, the further increase of C_d will affect the response in the

same manner that an increase of mass changes the response of a second order system.

It is noted that an increase in k_a (an increase in airspeed) serves to dampen the response still further. This was found to be true throughout both the linear and nonlinear analyses.

The gain of the system was doubled in Figs. V-1(D-F), and an optimum response of approximately .07 seconds was found for the system (the curve with the slight overshoot in Fig. V-1(E) is nearly the optimum response). Even with this higher gain, the effect of C_d as noticed before appears again. In Fig. V-1(G) we find a marginally stable response due to a high gain. Only one response was taken here because the low damping value caused the system to be completely unstable for all but the highest load value. Figs. V-1 (H-J) indicate that the high gain system can be stabilized by increasing the damping.

2) Nonlinear System Responses

The principal objective in studying the nonlinear system was to observe the effects of the various nonlinear elements on the system response, and to determine which, if any, could be satisfactorily neglected, or compensated for, in future analog computer studies.

It must be noted before any analysis of results is begun that the final value droop noticeable in many of the responses is not an actual system characteristic. It is, instead, the result of using extreme parameter values which overloaded certain of the computer components.

Fig. V-3(A-D) indicate that pressure feedback variations have little effect on the responses. The effect is slightly more noticeable at low k_a's due to the more oscillatory responses. It would seem, then, that the pressure feedback could be neglected for most practical system configurations. This is a valid assumption because it is unlikely that loop gain, damping, and other parameters would be set at values which would make the response oscillatory enough to make the feedback noticeable.

It should be understood that this feedback is not a deliberately constructed one; it is simply the transmission of pressure induced by load dynamics back to the valve orifices, and is inherent in any valve metered servo.

Figs. V-3(E-H) show that the addition of valve leakage provides damping for the system. This effect is most noticeable for the under lapped and low k_a conditions because these are the most oscillatory. Also, we may conclude that leakage and lap effects are small for high load conditions.

The effects of coulomb damping are illustrated in Figs. V-3(I-L). Coulomb damping influences the response quite radically for low load and viscous damping values. However, at conditions of higher viscous damping, the effect of coulomb damping is minimized and is practically negligible when higher loads are applied. This indicates that in an analysis such as this, coulomb damping can be compensated for by use of additional viscous damping.

Responses for various values of command step voltages are given in Figs. V-3(M-P). In this sort of test, the presence of nonlinear elements is most noticeable. It can be seen from these figures that the transients change greatly as the input level is changed. Percentage overshoot is plotted as a function of the input step in Fig. VI-1 (values for these curves were obtained with a calibrating line on the oscilloscope). The percentage overshoot is much higher for small inputs with a zero load. This is not so noticeable for higher loads, corresponding to actual operating conditions. It is seen, also, that the low input level instability is emphasized by a valve with underlap as shown in Fig. VI-1(A).

From the above, it may again be concluded that leakage provides damping. It may also be concluded from Figs. V-3 (M-T) that for a given value of leakage, the addition of underlap causes the system to become more oscillatory.

In observing the effects of changing the mass of the output member it was found that a mass increase caused the

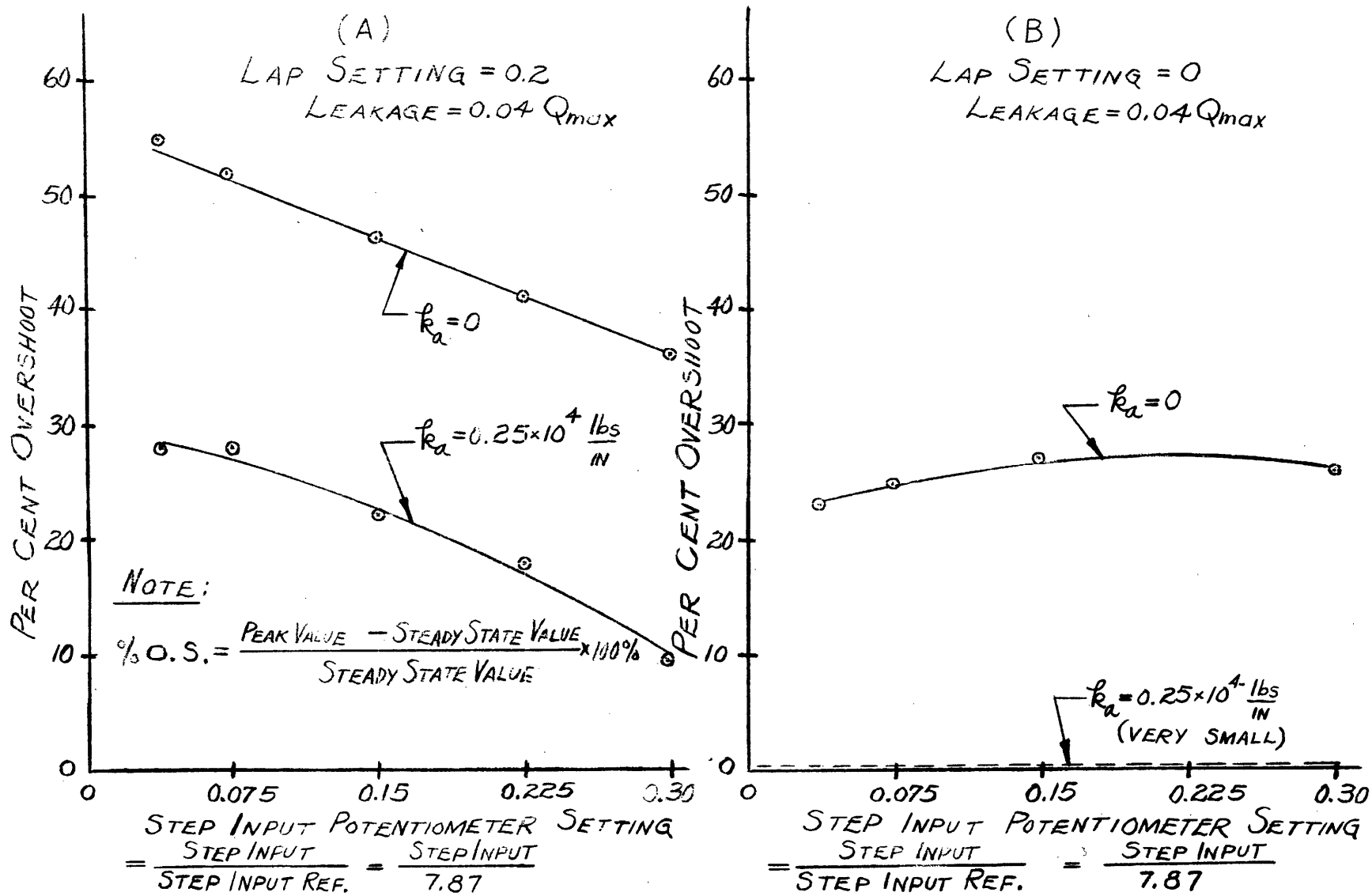

Fig. VI-1 Measured percent overshoot versus magnitude of step input

response to become much more oscillatory; decreasing the mass had the opposite effect. Since the output member mass is the coefficient on the p^3 term in the performance equation, it is difficult to predict how changes of this parameter would alter the response because this would require an investigation into the relative magnitudes of the other coefficients in the differential equation. Routh's criterion[13] might be used to determine absolute stability under various output member mass values, but any exact method of determining analytically the stability of a nonlinear system becomes quite involved. It is sufficient to state that under the conditions of operation inposed upon the system, higher output member masses brought on instability.

Fig. V-3(Y-Z) indicate that the removal of the viscous friction lumped at the actuator does not change the response appreciably. Addition of abnormal amounts of viscous friction, however, increases the overshoot and the response time; this can be observed in Figs. V-3 (AA-BB). Previous tests indicated the importance of viscous friction lumped at the elevator in system response.

The results of an investigation of the response of the system to an interfering step applied at the output member are shown in Figs. V-3 (CC-DD). The interfering input and the dynamic load are of opposite sign, and increasing the load tends to null out the final elevator displacement due to the interfering input. There is also an indication here that the addition of underlap adds damping to the system for interfering moment inputs. This is just opposite to the decreased damping effect of underlap for command voltage inputs.

3) Nonlinear System Responses (pick-off at elevator)

It was thought that substantially improved results might be obtained if the pick-off were located at the elevator instead of at the actuator. However, the responses were not materially improved, except that the aerodynamic load did not cause a constant error in elevator position as before.

The undamping effect of underlap is agian noticeable.

Photographs of the pressure feedback (Figs. V-4 (A-F) were taken here which illustrate the pressure induced by the load dynamics and transmitted back to the valve orifices.

4) Summary

With special regard toward future simulation studies of hydraulic servos, a few general conclusions may be made. Reference to Fig. IV-15 will show that a large number of electronic components are required to completely simulate this system, and any portions of the system which can be neglected will reduce the electronic equipment requirements. Two things which can be neglected are pressure feedback to the valve and coulomb damping if the system is not too oscillatory.

The valve is the most important of the nonlinear elements in the system. Leakage in the valve provides damping for the system, but underlap makes the response oscillatory. In simulating the valve, it was found that correctly balancing the valve was very critical. The slightest amount of unbalance in leakage resulted in a constant deflection of the output member for a zero command voltage.

An attempt was made to study the response of the system to very small command voltages and to evaluate the minimum command voltage for which an output could be measured. These voltages, however, were at the noise level of the computer and no definite conclusions could be reached.

B. Recommendations

The recommendations to be stated here are deemed necessary by the authors for one paramount reason: the element of time. While an effort has been made to make this report as complete and as all inclusive as possible, there was, nevertheless, the ever-present requirement to complete the report by "due-date". Given added time, the authors would have investigated the following problems; lacking this time, the authors present these problems as recommendations in the hope that they will be undertaken and explored in the future.

1) A more thorough study of the possibilities of system

optimization by means of the system's inherent nonlinearities (how can the leakage and lap of hydraulic servos be most advantageously utilized?).

2) An investigation of the hydraulic servo problem using an unbalanced valve (how will dither then affect the problem? will the effects of the nonlinearities be more pronounced?).

3) An investigation of the effects of hydraulic servo nonlinearities on a closed loop that includes aircraft dynamics. See Fig. VI-2 for a possible closed loop pitch rate control system employing the servo investigated in this report (the indicated system configuration was obtained from Reference 10; the relating functions for the various components may also be obtained from this reference).

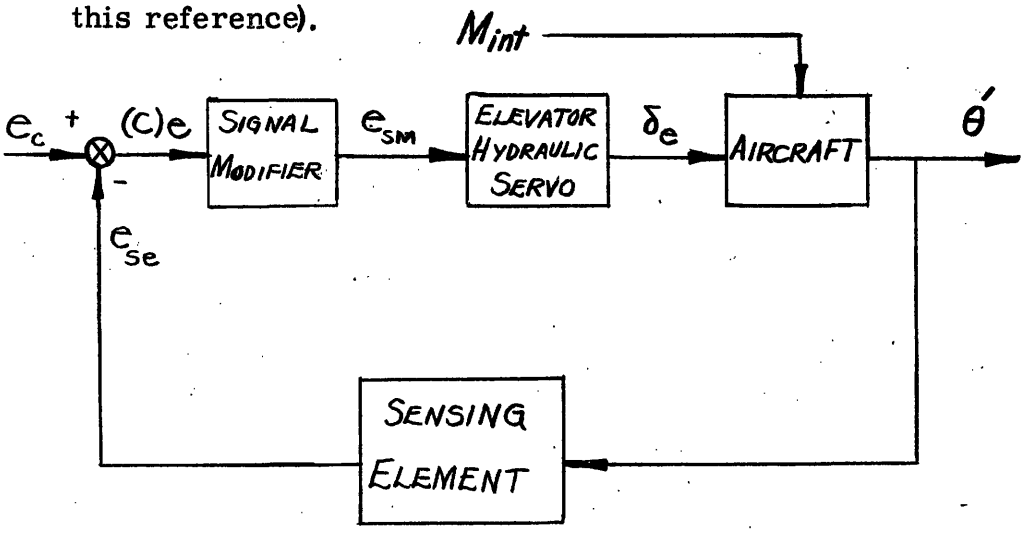

Fig. VI-2 Closed loop pitch rate control system

4) As an extension of 3 above, it is recommended that the effects of the hydraulic servo nonlinearities be investigated with the elevator dynamics included in, as well as out of, the elevator servo's feedback loop.

APPENDIX A

DEFINITIONS

A. Notation. The symbols and notations used in this report are, in general, based on the self-defining system developed by Draper. For a complete description of this method, the reader is referred to the works by that author[11]; for the purposes of this paper, however, the following brief explanation of the Draper self-defining notation system will suffice.

The relationship between two physically related quantities is represented symbolically as follows (Fig. A-1),

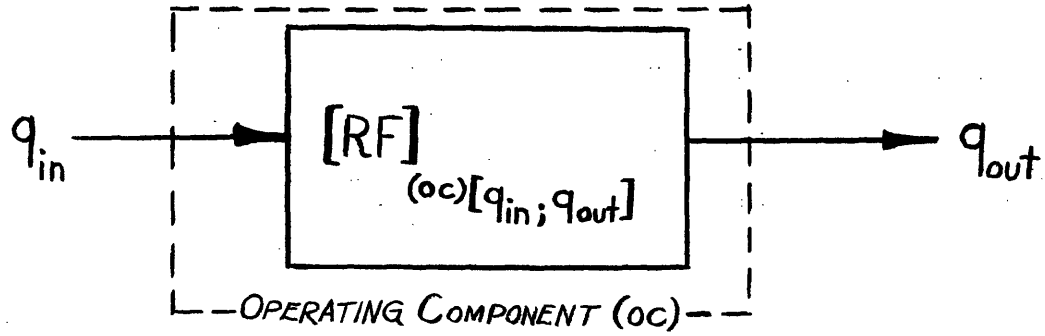

Fig. A-1 [RF] conventions

where $[RF]_{(oc)[q_{in};q_{out}]}$ = Relating Function of the operating component for q_{in} in and q_{out} out.

Note that the subscripts on $[RF]_{(oc)[q_{in};q_{out}]}$ fully describe the operating component in question: the subscripts in the first bracket describe the operating component (in this case "oc" means "operating component"), while the first and second subscripts in the second bracket, separated by a semicolon, describe the input and

output quantities respectively.

Mathematically, the relating function is defined as the ratio of the Laplace Transform[12] of the output quantitiy to the Laplace Transform of the input quantity, with the initial condition function (ICF) equal to zero (i.e., with all initial condition values of q_{in} and q_{out} to zero):

$$[RF]_{(oc)[q_{in};q_{out}]} = \frac{[LT]q_{out}}{[LT]q_{in}} = \frac{\int_0^\infty q_{out}\, e^{-pt}\, dt}{\int_0^\infty q_{in}\, e^{-pt}\, dt}\ ,\ (ICF) = 0 \qquad (A\text{-}1)$$

So that:

$$[LT]\ q_{out} = [RF]_{(oc)[q_{in};q_{out}]}\ [LT]\ q_{in} \qquad (A\text{-}2)$$

In general, the relating function is composed of the product of two terms, the static sensitivity $S_{(oc)[q_{in};q_{out}]}$ and the frequency function $[FF]$. The frequency function is a function of the Laplace Transform complex variable p, and describes the operating component's dynamics. The static sensitivity (generally a constant) is, by definition, the ratio of a small change between constant output levels to the corresponding small change between constant input levels; it carries the same subscripts as the $[RF]$*

$$[LT]q_{out} = [RF]_{(oc)[q_{in};q_{out}]}[LT]q_{in} = S_{(oc)[q_{in};q_{out}]}[FF][LT]q_{in} \qquad (A\text{-}3)$$

To illustrate the use of the preceding conventions, the analysis of the elevator dynamic system described in Chapter II, section A, is repeated here in somewhat greater detail.

From the schematic of this system, Fig. A-2, the differential equation describing the system's behavior is writted as

---

* The subscripts in the second-bracket are sometimes omitted when writing a static sensitivity.

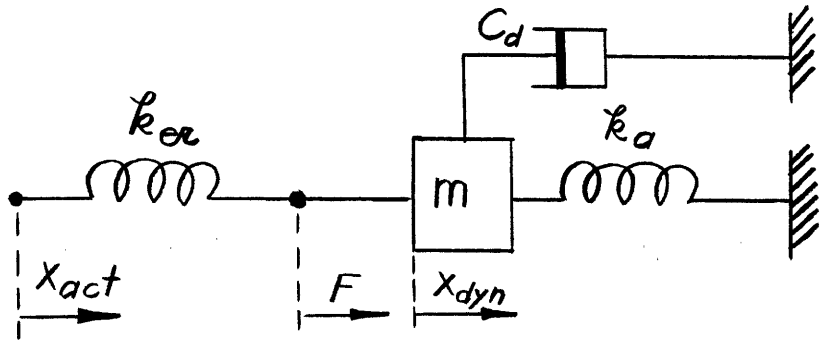

Fig. A-2 Elevator dynamic system (eds)

$$k_{er}(x_{act}-x_{dyn}) = m\frac{d^2x_{dyn}}{dt^2} + C_d\frac{dx_{dyn}}{dt} + k_a x_{dyn} \tag{A-4}$$

From which:

$$k_{er}[LT]\,x_{act} = [mp^2 + C_d p + k_a + k_{er}][LT]\,x_{dyn} \tag{A-5}$$

so that:

$$[RF]_{(eds)[x_{act};x_{dyn}]} = \frac{[LT]x_{dyn}}{[LT]x_{act}} = \frac{k_{er}}{mp^2+C_d p+k_a+k_{er}}$$

$$= \frac{k_{er}}{k_a+k_{er}}\left[\frac{1}{\frac{m}{k_a+k_{er}}p^2 + \frac{C_d}{k_a+k_{er}}p+1}\right] \tag{A-6}$$

$$= S_{(eds)[x_{act};x_{dyn}]}[FF] \tag{A-7}$$

also:

$$F = m\frac{d^2x_{dyn}}{dt^2} + C_d\frac{dx_{dyn}}{dt} + k_a x_{dyn} \tag{A-8}$$

so that:

$$[RF]_{(eds)[x_{dyn};F]} = \frac{[LT]F}{[LT]x_{dyn}} = mp^2 + C_d p + k_a$$

$$= k_a\left[\frac{m}{k_a}p^2 + \frac{C_d}{k_a}p+1\right]$$

$$= S_{(eds)[x_{dyn};F]}[FF] \tag{A-9}$$

further:

$$[RF]_{(eds)[x_{act};F]} = \frac{[LT]F}{[LT]x_{act}} = [RF]_{(eds)[x_{act};x_{dyn}]}[RF]_{(eds)[x_{dyn};F]}$$

$$= S_{(eds)[x_{act};x_{dyn}]} S_{(eds)[x_{dyn};F]} \left[\frac{1}{\frac{m}{k_a+k_{er}}p^2+\frac{C_d}{k_a+k_{er}}p+1}\right]\left[\frac{m}{k_a}p^2+\frac{C_d}{k_a}p+1\right]$$

$$= S_{(eds)[x_{act};F]}[FF] \qquad \text{(A-20)}$$

This final expression is represented symbolically as follows (Fig. A-3).

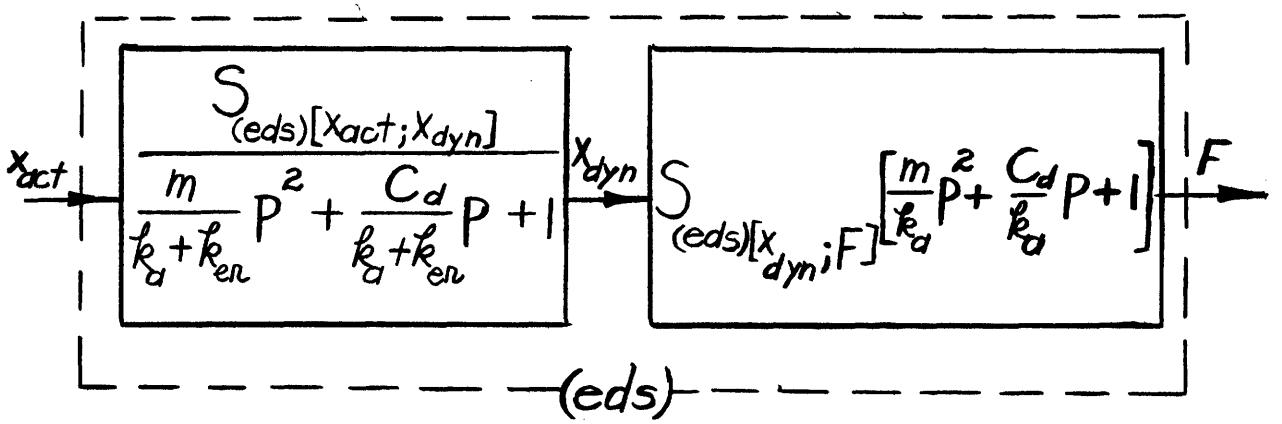

Fig. A-3 Relating Function of (eds)

B. Simulator Symbols. The following symbols are used in all simulator schematics of this report:

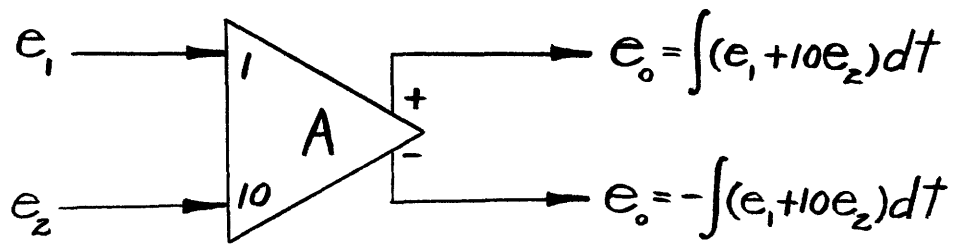

(a) Integrator symbol

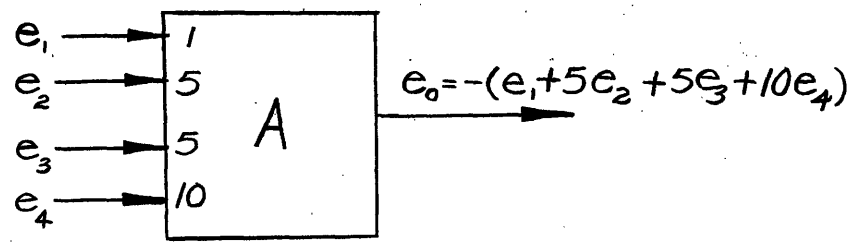

(b) Summing amplifier (Inverter) symbol

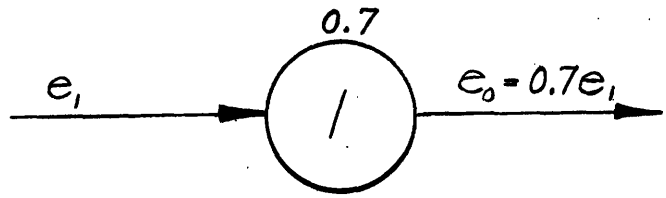

(c) Coefficient potentiometer symbol

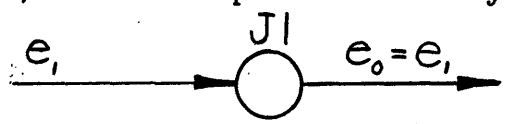

(d) Interpatch jack symbol

(e) Display jack symbol

Fig. A-4 Simulator symbols

To illustrate the use of these symbols, assume that the following problem is to be simulated on the GPS simulator:

$$\frac{d^2x}{dt^2} + 7.5\frac{dx}{dt} + 3x = f(t) \qquad \text{(A-11)}$$

Solve Eqn. (A-11) for the highest ordered derivative term

$$\frac{d^2x}{dt^2} = -7.5\frac{dx}{dt} - 3x + f(t) \qquad \text{(A-12)}$$

Assume next that $\frac{d^2x}{dt^2}$ is available at a point (Fig. A-5a); in order to

obtain this assumed quantity, generate the quantities $-7.5\frac{dx}{dt}$, $-3x$, and f(t) and couple these quantities to satisfy Eqn. (A-12). This is accomplished by the simulator arrangement indicated by Fig. A-5b. Note that this arrangement permits instantaneous observation of either of the quantities $\ddot{x}$, $\dot{x}$, x, or f(t).

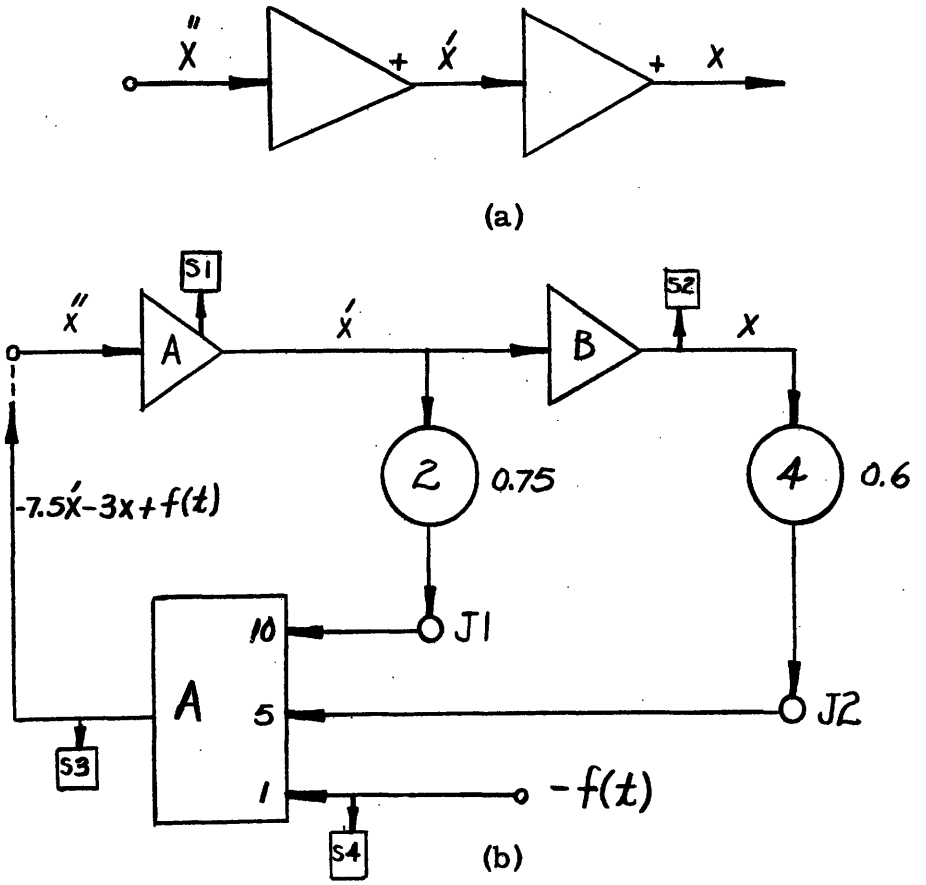

Fig. A-5 Illustrative simulator schematics

C. Units. The following definitions hold in this report:

Length	= x	=	inches (in)
Mass	= m	=	pounds per gravity (#/g)
Time	= t	=	seconds (sec)
Force	= F	=	pounds (#)
Torque	= T	=	pound-inches (#-in)
Pressure	= p	=	pounds per square inch (#/in)

Moment of inertia	= I	=	(pounds per gravity) times (inches squared) [(#/g)in^2] or, pounds-seconds squared-inches (#-sec^2-in), or slug in^2.
Angular momentum	= H	=	pounds-seconds-inches (#-sec-in)
Elastic coefficient	= k	=	pounds per inch (#/in) (lineal) or (pound-inches) per radian (#-in/rad) (rotational)
Rotation	= ω	=	radians per second (rad/sec)
Damping coefficient	= C_d	=	pounds per (inch per second), (#/in/sec), or, (#-sec/in)

APPENDIX B

GLOSSARY

A_{act}	Area of actuator piston
amp	Subscript notation for servo amplifier
as	Subscript notation for servo hydraulic actuator system
C	Magnitude of coulomb friction
$(C)_e = e_c - e_{po}$	Servomechanism correction voltage
c_d	Equivalent rotational viscous friction coefficient
C_d	Equivalent linear viscous friction coefficient
C_{d_1}	Coefficient of viscous friction lumped at hydraulic actuator
C_{d_2}	Coefficient of viscous friction lumped at servo elevator
e_c	Servomechanism command voltage
e_{po}	Servomechanism pick-off voltage
eds	Subscript notation for elevator dynamic system
els	Subscript notation for elevator linkage system
f_n	Undamped natural frequency
F	Force
g=32.2 ft/sec	Acceleration due to gravity
h	Ratio of fluid pressure to fluid density (pressure head)
I	Moment of inertia of elevator about elevator hinge line

i_{amp}	Servo amplifier output current
k	Torque at elevator hinge line due to an applied elevator deflection
$K = \frac{\Delta V}{\Delta P}$	Bulk modulus of hydraulic fluid
k_a	Coefficient of aerodynamic restraint
k_{er}	Linkage elastic restraint coefficient
k_{hyd}	Equivalent elastic restraint coefficient of hydraulic lines
m	Reflected elevator equivalent mass
M_{eh}	Moment at elevator hinge line
p	Hydraulic pressure Complex Laplace Transform variable (Context makes usage clear)
p_L, P_L	Hydraulic load pressure
P_r	Hydraulic return pressure
p_s, P_s	Hydraulic supply pressure
po	Subscript notation for servo pick-off
Q_c	Hydraulic flow rate loss due to compression of hydraulic fluid
$Q_{net} = Q_v - Q_c$	Net effective hydraulic flow rate
$Q_{n.l.}$	No load hydraulic flow rate
Q_v	Hydraulic flow rate from valve
$[RF]_{(oc)[q_{in};q_{out}]}$	Relating Function of operating component, for q_{in} in and q_{out} out (see Appendix A)
$S_{act} = \frac{1}{A_{act}}$	Servo hydraulic actuator sensitivity
S_{amp}	Servo amplifier sensitivity
S_{els}	Elevator linkage system sensitivity
S_{po}	Servo pick-off sensitivity
S_v	Hydraulic valve sensitivity
t	Time

v	Velocity of hydraulic fluid through an orifice Subscript notation for servo hydraulic valve (Context makes usage clear)
V_c	Volume of hydraulic fluid due to compression
V_v	Volume of hydraulic fluid from valve
x_{act}	Linear displacement of actuator
x_{dyn}	Dynamic linear displacement
δ_e	Angular deflection of elevator
$\triangle q$	Incremental change of quantity q
ρ	Hydraulic fluid density
θ'	Aircraft rate of pitch
ω_n	Undamped natural angular velocity
ζ	Damping ratio
$\dot{q} = \frac{dq}{dt}$	Time rate of change of quantity q

APPENDIX C

B IBLIOGRAPHY

1. "Hydraulic Servos Incorporating a High-Speed Hydraulic-Amplifier Actuated Valve", R. L. Scrafford. Applications and Industry, American Institute of Electrical Engineers, New York, N.Y., no. 7, July 1953, pp. 175-180.

2. "Fundamental Aspects of a Hydraulic-Type-Powered Flight-Control System", H. M. DeGroff, R. C. Binder, J. G. Truxal, and J. R. Burnett. Aeronautical Engineering Review, Institute of the Aeronautical Sciences, New York, N.Y., vol. 11, November, 1952, pp. 42-55.

3. "Optimization of Nonlinear Control Systems by Means of Nonlinear Feedbacks", R. S. Neiswander, and R. H. MacNeal. Applications and Industry, American Institute of Electrical Engineers, New York, N.Y., no. 8, September, 1953, pp. 262-272.

4. "Nonlinear Techniques for Improving Servo Performance", D. McDonald. Proceedings, National Electronics Conference, Chicago, Illinois, vol. 6, 1950, pp. 400-21.

5. "Describing Function Method of Servomechanism Analysis Applied to Most Commonly Encountered Nonlinearities", H. D. Grief. Applications and Industry, American Institute of Electrical Engineers, New York, N.Y., no. 8, September, 1953, pp. 243-248.

6. "The Use of Nonlinear Feedback to Improve the Transient Response of a Servomechanism", J. B. Lewis. Transactions, American Institute of Electrical Engineers, vol. 71, part II, 1953, pp. 449-453.

7. Elementary Fluid Mechanics (book), J.K. Vennard. John Wiley and Sons, New York, N.Y., 1950.

8. Servomechanism and Regulating System Design, vol. 1 (book), H. Chestnut and R.W. Mayer. John Wiley and Sons, New York, N.Y., 1951.

9. An All Electronic High Speed Multiplier,(report), S. Giser. Instrumentation Laboratory report no. R-67, Massachusetts Institute of Technology, Cambridge, Massachusetts, November, 1953.

10. Recent Developments in Aircraft Control, (paper), R.C. Seamans, F.A. Barnes, V.W. Howard, and T.B. Garber. Institute of the Aeronautical Sciences, New York, N.Y., I.A.S. Preprint no. 459, January 27, 1954.

11. Instrument Engineering, vols. 1 and 2 (book), C.S. Draper, W. McKay, and S. Lees. Mc-Graw-Hill Co., New York, N.Y., 1952.

12. Advanced Calculus for Engineers,(book), F.B. Hildebrand. Prentice-Hall, Inc., New York, N.Y., 1949.

13. Principles of Servomechanisms, (book), G.S. Brown, and D.P. Campbell. John Wiley and Sons, New York, N.Y., 1948.

14. "Analogies for Hydraulic and Electrical Drives in Servomechanisms", Yaohan Chu, and L.A. Gould. Transactions, American Society of Mechanical Engineers, New York, N.Y., July, 1953, no. 75:851-7.

15. "The Effects of Backlash and of Speed-Dependent Friction on the Stability of Closed-Cycle Control Systems", A. Tustin. Journal, Institution of Electrical Engineers, London, England, vol. 94, part IIA, 1947, pp. 143-51.